Science of the Total Environment 521–522 (2015) 431–445

Contents lists available at ScienceDirect

Science of the Total Environment

journal homepage: www.elsevier.com/locate/scitotenv

Carbonaceous aerosols and pollutants over Delhi urban environment: Temporal evolution, source apportionment and radiative forcing

D.S. Bisht [a], U.C. Dumka [b,*], D.G. Kaskaoutis [c], A.S. Pipal [d], A.K. Srivastava [a], V.K. Soni [e], S.D. Attri [e], M. Sateesh [e], S. Tiwari [a]

[a] Indian Institute of Tropical Meteorology, New Delhi, India
[b] Aryabhatta Research Institute of Observational Sciences, Nainital, India
[c] School of Natural Sciences, Shiv Nadar University, Tehsil Dadri, India
[d] Department of Chemistry, Savitribai Phule Pune University, Pune, India
[e] India Meteorology Department, Lodhi Road, New Delhi, India

HIGHLIGHTS

- Very high $PM_{2.5}$ (>200 μg m^{-3}) levels over Delhi during agricultural burning period.
- Enhanced levels of carbonaceous, sulphate and nitrate aerosol.
- OC/EC suggests dominance of biomass burning and SOA formation.
- BC highly contributes (50~70%) to the aerosol radiative forcing.

ARTICLE INFO

Article history:
Received 17 December 2014
Received in revised form 21 February 2015
Accepted 20 March 2015
Available online 8 April 2015

Editor: Xuexi Tie

Keywords:
$PM_{2.5}$
Carbonaceous aerosols
Inorganic ions
Agricultural burning
Radiative impact
Delhi

ABSTRACT

Particulate matter ($PM_{2.5}$) samples were collected over Delhi, India during January to December 2012 and analysed for carbonaceous aerosols and inorganic ions (SO_4^{2-} and NO_3^-) in order to examine variations in atmospheric chemistry, combustion sources and influence of long-range transport. The $PM_{2.5}$ samples are measured (offline) via medium volume air samplers and analysed gravimetrically for carbonaceous (organic carbon, OC; elemental carbon, EC) aerosols and inorganic ions (SO_4^{2-} and NO_3^-). Furthermore, continuous (online) measurements of $PM_{2.5}$ (via Beta-attenuation analyser), black carbon (BC) mass concentration (via Magee scientific Aethalometer) and carbon monoxide (via CO-analyser) are carried out. $PM_{2.5}$ (online) range from 18.2 to 500.6 μg m^{-3} (annual mean of 124.6 ± 87.9 μg m^{-3}) exhibiting higher night-time (129.4 μg m^{-3}) than daytime (103.8 μg m^{-3}) concentrations. The online concentrations are 38% and 28% lower than the offline during night and day, respectively. In general, larger night-time concentrations are found for the BC, OC, NO_3^- and SO_4^{2-}, which are seasonally dependent with larger differences during late post-monsoon and winter. The high correlation ($R^2 = 0.74$) between OC and EC along with the OC/EC of 7.09 (day time) and 4.55 (night-time), suggest significant influence of biomass-burning emissions (burning of wood and agricultural waste) as well as secondary organic aerosol formation during daytime. Concentrated weighted trajectory (CWT) analysis reveals that the potential sources for the carbonaceous aerosols and pollutants are local emissions within the urban environment and transported smoke from agricultural burning in northwest India during post-monsoon. BC radiative forcing estimates result in very high atmospheric heating rates (~1.8–2.0 K day^{-1}) due to agricultural burning effects during the 2012 post-monsoon season.

1. Introduction

Carbonaceous aerosols (elemental carbon, EC; or equivalent black carbon, BC; organic carbon, OC) constitute a large fraction (~20 to 70%) of atmospheric aerosols and play a crucial role in the visibility degradation, formation of haze, atmospheric heating and adverse human health (Seinfeld and Pandis, 1998; Ramanathan and Carmichael, 2008; Chung et al., 2012; Ancelet et al., 2013; Pachauri et al., 2013). EC, as primary pollutant, is emitted from incomplete combustion of biomass burning, fossil fuel and carbon-contained materials and, due to its strong absorbing nature, is the most important driver to aerosol-induced global warming (Hansen et al., 2005; Bollasina et al., 2011; Bond et al., 2013) enhancing the melting of Himalayan

* Corresponding author.
E-mail addresses: dumka@aries.res.in, ucdumka@gmail.com (U.C. Dumka).

http://dx.doi.org/10.1016/j.scitotenv.2015.03.083
0048-9697/

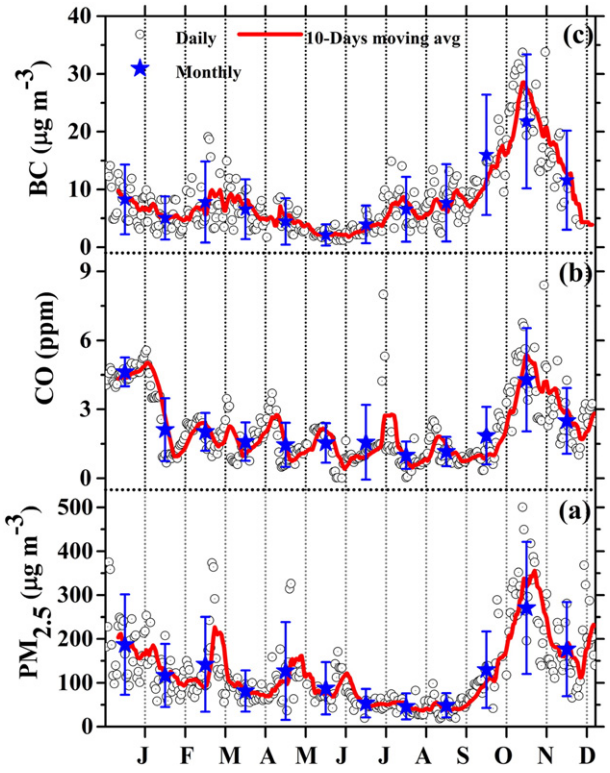

Fig. 1. Temporal evolution of daily-mean online measurements of $PM_{2.5}$ mass concentration (a), carbon monoxide (b) and BC mass concentration (c) during January to December 2012. The ten-day moving average along with monthly means are also shown. The vertical bars correspond to one standard deviation from the monthly mean.

glaciers via deposition over the snow and ice packs (Menon et al., 2010; Kaspari et al., 2011). On the other hand, OC, which is scattering rather than absorbing in nature, is directly released into the atmosphere from combustion and/or biogenic sources (primary OC; POC) or produced from gas-to-particle conversion of volatile organic compounds (secondary OC; SOC) (Pandis et al., 1992; Turpin and Huntzicker, 1995; Satsangi et al., 2012). OC can be also a mixture of several organic compounds, such as polycyclic aromatic hydrocarbons (PAHs), polychlorinated dibenzo-p-dioxins and dibenzofurans (PCDD/Fs) some of which being carcinogenic in nature (Li et al., 2008; Feng et al., 2009). Recent studies (Andreae and Gelencsér, 2006; Bahadur et al., 2012; Chung et al., 2012) have shown that OC may also have a strong absorbing tendency in the UV-to-visible spectrum and significant influence on the aerosol radiative forcing (ARF).

Carbonaceous aerosols, either from human or natural emissions, are very abundant over Indian sub-continent and adjoining oceanic regions contributing to formation of the Atmospheric Brown Clouds (ABC) and Asian pollution outflow (Ramanathan et al., 2005, 2007; Lawrence and Lelieveld, 2010 and references therein). Due to their important role in degradation of visibility, formation of haze and fog over Ganges Basin, heating of the lower and mid-tropospheres and melting of Himalayan glaciers, carbonaceous aerosols and gases in the form of OC, BC, CO are systematically examined over India (Babu and Moorthy, 2002; Tripathi et al., 2005; Venkataraman et al., 2005; Rengarajan et al., 2007; Satsangi et al., 2010; Ram and Sarin, 2010, 2011, 2015; Sharma et al., 2010; Ram et al., 2012; Bisht et al., 2013; Dumka et al., 2013; Verma et al., 2013; Tiwari et al., 2013a, 2014a; Pipal et al., 2014a,b; Gadhavi et al., 2014; Safai et al., 2014; Srivastava et al., 2014) via multiple ground-based instrumentation and techniques as well as satellite remote sensing. The climatic response of carbonaceous aerosols on the weakening of the summer Indian monsoon has attracted the global scientific interest (Meehl et al., 2008; Cowan and Cai, 2011) and current modelling approaches deal with this issue over south Asia and Tibetan Plateau (Lau et al., 2006; Randles and Ramaswamy, 2008; Ganguly et al., 2012).

The current work examines a year-long (Jan–Dec 2012) set of Particulate Matter < 2.5 μm ($PM_{2.5}$) concentrations in the Delhi urban environment, which are analysed for the carbonaceous species (OC, EC) along with inorganic ions (SO_4^{2-} and NO_3^-). Furthermore, continuous real-time measurements of $PM_{2.5}$, BC mass concentration and CO support the analysis by providing the diurnal patterns, daily, monthly and seasonal averages. The main objectives of the current work are i) to improve the current knowledge of carbonaceous aerosols and pollutants over Delhi during a year with severe post-monsoon biomass burning, ii) to quantify the relative contribution of OC/EC in $PM_{2.5}$, iii) to understand the seasonality of carbonaceous aerosols and the relative importance of primary versus secondary OC sources, iv) to reveal the hotspot areas that mostly contribute to the high carbonaceous aerosol concentrations and, v) to examine the impact of BC on radiative forcing. In this respect, the current work uses various instrumentation and techniques and provides an extensive literature overview of the OC, EC and OC/EC over urban, rural, remote and elevated sites over the globe.

2. Site description and measurement set up

90 (45 for daytime and 45 for night-time) $PM_{2.5}$ samples were collected during January to December 2012 (3–5 samples per month) on

Table 1
Seasonal-mean concentrations of $PM_{2.5}$, OC, EC, BC, SO_4^{2-} and NO_3^- over Delhi during day and night. The seasons are classified as follows: winter (December–January); pre-monsoon (March–June); monsoon (July–September) and post-monsoon (October–November).

Months	$PM_{2.5}$ offline	OC μg m^{-3}	EC μg m^{-3}	OC/EC μg m^{-3}	SO_4^{2-} μg m^{-3}	NO_3^- μg m^{-3}	$PM_{2.5}$ online	BC μg m^{-3}	CO ppm
Day time (10:00 to 18:00 h local time)									
Winter	204.15 ± 23.93	46.28 ± 8.22	7.27 ± 2.20	6.72 ± 1.48	31.09 ± 10.65	13.05 ± 8.14	146.28 ± 83.02	6.29 ± 4.01	3.09 ± 1.07
Summer	157.39 ± 47.19	24.60 ± 6.67	3.45 ± 1.43	7.76 ± 2.03	20.05 ± 15.05	9.67 ± 11.23	90.22 ± 21.73	2.22 ± 1.35	1.40 ± 0.70
Monsoon	115.13 ± 27.13	26.42 ± 7.14	3.73 ± 1.01	7.33 ± 1.87	17.04 ± 7.81	7.48 ± 5.66	37.40 ± 13.65	3.83 ± 1.46	0.74 ± 0.42
Post-monsoon	199.44 ± 41.55	46.58 ± 12.06	8.34 ± 2.89	6.10 ± 2.05	33.73 ± 11.90	22.88 ± 6.48	168.04 ± 72.14	11.66 ± 3.94	2.65 ± 1.40
Night time (19:00 to 07:00 h local time)									
Winter	250.81 ± 25.98	62.42 ± 11.60	14.06 ± 3.60	4.72 ± 1.21	32.33 ± 11.68	19.79 ± 7.94	216.85 ± 85.61	12.77 ± 5.86	3.68 ± 1.46
Summer	155.34 ± 49.52	30.34 ± 16.97	8.54 ± 6.41	4.01 ± 1.69	13.31 ± 7.42	5.68 ± 5.97	82.32 ± 50.49	7.70 ± 7.25	1.80 ± 0.89
Monsoon	100.86 ± 17.76	26.89 ± 8.15	4.65 ± 1.65	6.10 ± 1.86	10.84 ± 4.60	6.52 ± 2.10	35.25 ± 12.77	6.30 ± 2.91	0.82 ± 0.37
Post-monsoon	234.83 ± 35.35	53.50 ± 12.11	15.75 ± 1.93	3.39 ± 0.56	37.15 ± 13.02	28.60 ± 8.25	228.86 ± 102.55	19.44 ± 4.65	3.11 ± 1.38
All data									
Day	164.16 ± 39.93	34.05 ± 11.66	5.29 ± 2.37	7.15 ± 1.23	23.66 ± 9.12	12.15 ± 6.79	103.80 ± 57.89	5.2 ± 3.83	1.81 ± 1.06
Night	179.02 ± 64.80	41.40 ± 17.62	10.30 ± 5.69	4.58 ± 1.46	21.29 ± 12.18	13.34 ± 10.12	129.39 ± 90.59	10.59 ± 6.75	2.18 ± 1.27
Total	171.59 ± 51.61	37.73 ± 14.32	7.79 ± 3.73	5.86 ± 0.99	22.47 ± 10.23	12.74 ± 8.18	116.57 ± 73.19	7.89 ± 5.14	1.99 ± 1.16

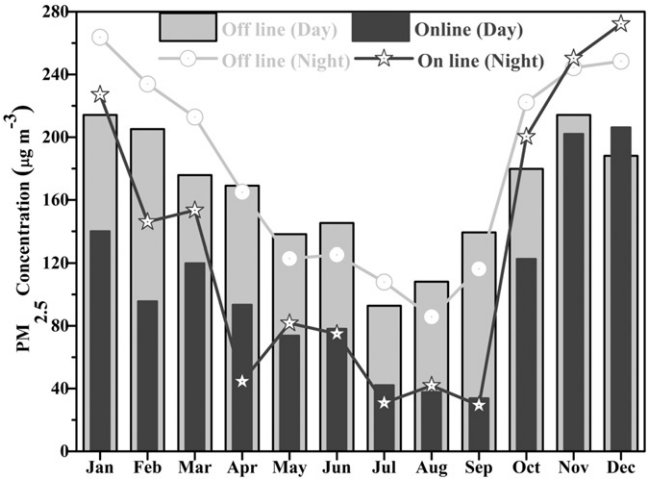

Fig. 2. Monthly-mean variation of online and offline $PM_{2.5}$ mass concentrations during day and night.

the rooftop of a building (~15 m a.g.l) in the premises of Indian Institute of Tropical Meteorology, New Delhi Branch (28.35° N; 77.12° E; 217 m a.m.s.l). Delhi is situated between the rich rain-washed Indo-Gangetic Plain (IGP) in the east and the semi-arid tracts of Rajasthan to the southwest and is one of the most densely populated and aerosol-polluted urban environments over the globe (Tiwari et al., 2013b). The major sources of anthropogenic pollution consist of emissions from power plants, transportation, small-scale industries and domestic cooking in addition to seasonal agricultural biomass burning and dust storms (Lodhi et al., 2013). The site is characterized by a semi-arid type of climate, with high summer-monsoon (July–September) rainfall and dryness during the pre- (March–June) and post-monsoon (October–November) periods, while winter (December–February) is chilly, foggy and with scarce rainfall in view of thunderstorms (Tiwari et al., 2010; Srivastava et al., 2014). Winds are in general low (2–5 ms^{-1}), blowing from southeast directions during monsoon to northwest during the rest of the year influencing aerosol sources, types and transport pathways (Lodhi et al., 2013).

3. Instrumentation, measurements and techniques

Two sets of measurements using different instrumentation and techniques are utilized in the present work. More specifically, aerosol sampling was carried out using a single stage APM-550 medium volume air sampler (gravimetric: off-line; Envirotech Pvt. Ltd., India) for $PM_{2.5}$ mass recordings based on impactor designs standardized by USEPA (United States Environmental Protection Agency). The APM-550 is supplied with a Dry Gas Meter to provide a direct measure of the total volume of air, while the sampling rate is held constant at 1 m^3 h^{-1} by a suitable critical orifice. Ambient air enters the APM 550 samplers through an omni-directional inlet designed to provide a clean aerodynamic cut-point for particles greater than 10 μm. PM_{10} concentrations proceed to a second impactor with an aerodynamic cut-point at 2.5 μm and the $PM_{2.5}$ mass is passed through a 47 mm diameter Quartz fibre filter membrane that retains the fine PM. The filters were subjected to desiccation for 24 h before and after the sampling in order to remove the moisture content and then, were weighted using the electronic microbalance (Model GR202, A&D Com. Japan; http://scaleman.com/semi-microbalance-analytical-weighing.html) with a high accuracy of 0.001 mg. The aerosol mass concentrations were determined gravimetrically by the difference in the weights before and after sampling. The exposed filter papers were then analysed for OC and EC concentrations by semi-continuous thermal/optical carbon analyser (Sunset Laboratory Inc. Model 4 L: http://www.sunlab.com) using the NIOSH 5040 (National Institute for Occupational Safety and Health) protocol (Birch and Cary, 1986). An aliquot of sample filter (2.1 cm^2) was stepwise heated in a furnace up to 840 °C in a non-oxidizing atmosphere (100% He); furnace was then cooled to 550 °C and the filter was stepwise heated to 850 °C in an oxidizing atmosphere (90% He, 10% O_2). During each temperature step, evolved carbon was converted to methane and detected by a flame ionization detector. Calibration was performed at the end of each analysis by introducing a known amount of methane into the oven and measuring its constant response. The carbon evolved before split line is considered as OC, whereas that evolved after the split line is quantified as EC (Tiwari et al., 2013a). Analysis of inorganic ions (NO_3^- and SO_4^{2-}) was performed via the Reagent Free Ion Chromatograph (IC: DIONEX-2000, RFIC, make; USA) and details are presented elsewhere (Tiwari et al., 2009). The APM-550 samples and gravimetric analysis were performed once per week with sampling times of 8

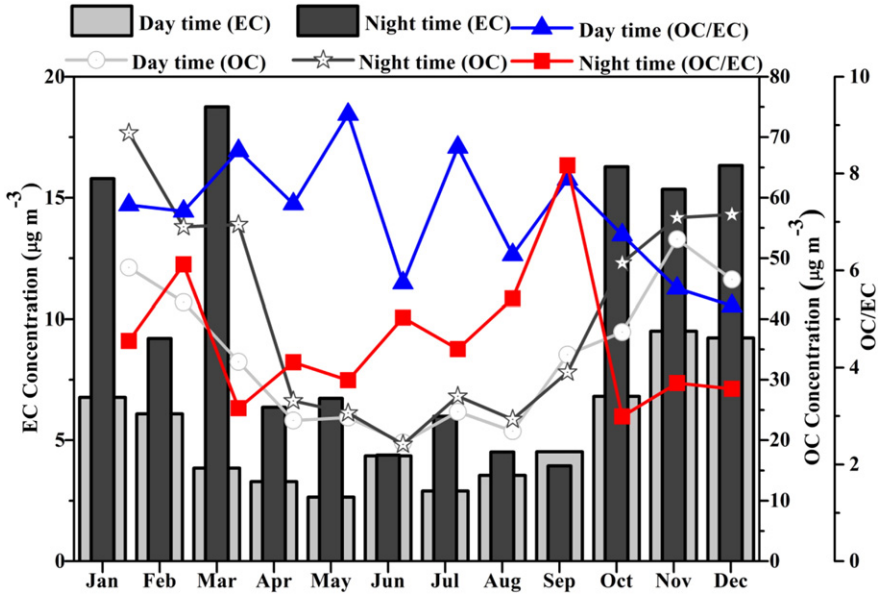

Fig. 3. Monthly-mean variation of EC, OC and OC/EC during day and night obtained via offline measurements.

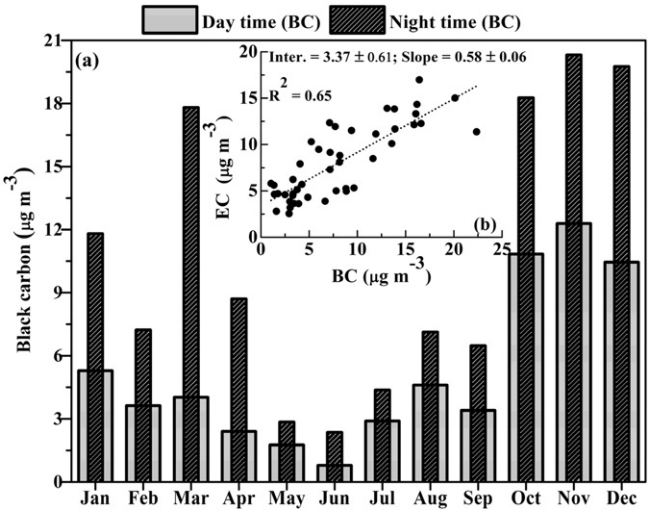

Fig. 4. Monthly-mean variation of BC mass concentration (online measurements) during day and night and correlation with EC (inset graph).

(10:00–18:00 h) and 12 (19:00–07:00 h) hours during day and night times, respectively.

Furthermore, $PM_{2.5}$ mass concentrations were carried out via Beta-attenuation analyser (Thermo Andersen, Inc. USA; series FH 62 C14) with temporal resolution of 5 min. The 2.5 μm size cut-off was achieved through a sharp-cut cyclone inlet with a flow rate of 1 $m^3\ h^{-1}$. The instrument's measuring range is 0–5000 μg m^{-3} with a minimum detection limit of 1 μg m^{-3} for 24-h average (Kenny et al., 2000; Hyvärinen et al., 2009; Tiwari et al., 2014b). These $PM_{2.5}$ recordings are named "online" instead of the "offline" gravimetric measurements and are used for examining the diurnal pattern of $PM_{2.5}$. Moreover, BC mass concentrations (temporal resolution of 5 min) were estimated via a seven-wavelength portable Aethalometer (Model AE-31, Magee Scientific USA; http://www.mageescientific.com) from the light attenuation at 880 nm using a specific mass absorption coefficient of 16.6 $m^2\ g^{-1}$ (Babu and Moorthy, 2002; Dumka et al., 2013). Carbon monoxide (CO) was measured directly by CO analyser (Model 49i, Thermo Scientific, USA) with a temporal resolution of 5 min (Tiwari et al., 2014b).

For examining source apportionment of $PM_{2.5}$ and carbonaceous aerosols, 5-day isentropic air-mass back trajectories were obtained over Delhi at 500 m agl via the Hybrid Single Particle Lagrangian Integrated Trajectory (HYSPLIT) model (Draxler et al., 2014; http://ready.arl.noaa.gov/HYSPLIT.php). The Concentrated Weighted Trajectory (CWT) analysis was used to quantify the regional contribution of each of advection pathway to the measured aerosol variable (Seibert et al., 1994; Dumka et al., 2013). The trajectories ending at 500 m over Delhi were weighted on the basis of the measured properties ($PM_{2.5}$, OC, BC, EC, SO_4^{2-}, NO_3^- and CO) during their arrival and each grid cell was assigned a concentration obtained by averaging trajectory-associated concentrations that had crossed the grid cell:

$$C_{ij} = \frac{1}{\sum_{l=1}^{N} \tau_{ijl}} \sum_{l=1}^{N} C_l \tau_{ijl} \quad (1)$$

where C_{ij} is the average weighted concentration in a grid cell (i, j), C_l the measured variable, τ_{ijl} the number of lth trajectory endpoints in the (i, j) grid cell and N the total number of trajectory endpoints in (i, j) grid (Seibert et al., 1994).

Table 2
EC and OC concentrations at Delhi and those from the other sites from globe.

Location	Size	Type of location	Period	OC (μg m^{-3})	EC (μg m^{-3})	OC/EC	References
Delhi	$PM_{2.5}$	Urban (217 m amsl)	Jan–Dec 2012 (day time)	34.1 ± 11.7	5.3 ± 2.3	7.09 4.55	Present study
			Jan–Dec 2012 (night time)	41.4 ± 17.6	10.3 ± 5.7		
Delhi	$PM_{2.5}$	Urban	Jan–Dec 2010	26.7 ± 9.2	6.1 ± 3.9	4.38	Sharma et al. (2014)
Delhi	$PM_{2.5}$	Urban	Jan-2011–May-2012	23 ± 16	11 ± 7	2.2 ± 0.5	Srivastava et al. (2014)
Agra, India	$PM_{2.5}$	Suburban	May 2010–Apr 2011	22.8	3.4	6.6	Pachauri et al. (2013)
Agra India	$PM_{2.5}$	Dayalabagh University Campus	Nov 2010–Feb 2011	44.5 ± 18.5	5.0 ± 1.4	8.1	Pachauri et al. (2013)
Ahmedabad, India	$PM_{2.5}$	Urban	Dec 2006–Jan 2007	18.3 ± 5.9	3.0 ± 0.9	6.2 ± 0.8	Rengarajan et al. (2011)
Kanpur, India	$PM_{2.5}$	Urban	Oct 2008	47.0	7.7		Ram and Sarin (2010)
Hong Kong	$PM_{2.5}$	Urban	2004–2005	7.42 ± 1.22	6.01 ± 0.55		So et al. (2007)
Hong Kong	$PM_{2.5}$	Urban	winter 2005	13.4 ± 6.2	2.3 ± 0.8	6.4 ± 3.2	Duan et al. (2007)
Kaohsiung, Taiwan	$PM_{2.5}$	Urban	Nov 1998–Apr 1999	10.5 ± 4.8	4.08 ± 1.82	2.56 ± 1.64	Lin (2002)
Shanghai, China	$PM_{2.5}$	JD (Suburban)	Oct 2005–Aug 2006	17.4	3.1	5.6	Feng et al. (2009)
Beijing, China	$PM_{2.5}$	AES (suburban)	July, Nov 2002	25.6	5.6	4.6	Feng et al. (2006)
Guangzhou	$PM_{2.5}$	LG (suburban)	Dec 2002, July 2003	22.6	6.5	3.5	Feng et al. (2006)
Nanjing, China	$PM_{2.5}$	PMO (suburban)	Feb 2001	14.2	2.9	4.9	Yang et al. (2005)
Tianjin, China	$PM_{2.5}$	Urban	Jan, April, July 2007	23.2	5.1	4.4	Li and Bai (2009)
Wusumu, China	$PM_{2.5}$	Semi-arid	2005–2007	11.8	1.8		Han et al. (2008)
Xiamen, China	$PM_{2.5}$	Jimei University	Jan 2010	28.9 ± 4.3	4.5 ± 0.04	6.5 ± 1	Zhang et al. (2012)
Changchun, China	$PM_{2.5}$	Jilin University	Jan 2003	39.2 ± 8.7	13.5 ± 2.9	2.9	Cao et al. (2007)
Guangzhou, China	$PM_{2.5}$	Zhongshan University	Jan 2003	41.1 ± 29.6	14.5 ± 9.9	2.8	Cao et al. (2007)
Wushan, Guangzhou, China	$PM_{2.5}$	Institute of Geochemistry, Chinese Academy of Science	Feb–Mar 2005	23.9 ± 19.9	4.4 ± 2.2	5.0	Duan et al. (2007)
Beijing China	$PM_{2.5}$	Tsinghua University	Nov 1999–Mar 2000	31.49	11.08		He et al. (2001)
Guangzhou, GZ	$PM_{2.5}$	Urban	2006–2007 Winter	8.53	4.81		Huang et al. (2012)
			2006–2007 Summer	5.97	3.46		
Singapore	$PM_{2.5}$	Urban	Mar 2001–Mar 2002	3.45 ± 1.67	1.78 ± 1.13	1.94 ± 1.55	See et al. (2006)
Singapore	$PM_{2.5}$	National University Campus	Jan–Dec 2000	7.34	3.26		Balasubramanian et al. (2003)
Milan, Italy	$PM_{2.5}$	Urban	2002–2003	9.6	1.4	6.9	Lonati et al. (2007)
Helsinki, Finland	$PM_{2.5}$	Urban	July 2001–2001	3.0	1.1	2.6	Viidanoja et al. (2002)
Yokohama, Japan	$PM_{2.5}$	Urban	Sept 2007–Aug 2008	3.75	1.94	1.9	Khan et al. (2010)
Gwangju, Korea	$PM_{2.5}$	University Campus	Nov 2008–Feb 2009	2.13–19.52	0.67–10.1	1.4–7.9	Park and Cho (2011)
Lahore Pakistan	$PM_{2.5}$	University of Engineering & Technology campus	Nov 2007–Jan 2008	85.7–152	13.8–21		Stone et al. (2010)

4. Results and discussion

4.1. $PM_{2.5}$ concentrations over Delhi

Continuous $PM_{2.5}$ measurements (online) were carried out in Delhi during January to December 2012 exhibiting a remarkable daily, monthly and seasonal variability (Fig. 1a, Table 1) with an annual mean of 124.6 ± 87.9 μg m^{-3} and range from 18.2 ± 6.87 μg m^{-3} (06th September 2012) to 500.6 ± 197.4 μg m^{-3} (07th November 2012). The daily as well as the seasonal and annual $PM_{2.5}$ concentrations are far beyond the annual standards of 40 μgm^{-3} stipulated by the Central Pollution Control Board (CPCB), named National Ambient Air Quality Standard (NAAQS) (http://www.cpcb.nic.in/National-Ambient-Air-Quality-Standards.php), and ~6–7 times above the USEPA (15 μg m^{-3}: http://www.epa.gov/air/criteria.html) and European Union (20 μg m^{-3}: http://ec.europa.eu/environment/air/quality/standards.htm) standards, rendering Delhi as one of the most heavily aerosol-laden environments over the globe, comparable in magnitude to windy dusty environments in southwest Asia (Rashki et al., 2012).

$PM_{2.5}$ concentrations present much lower values and variability during the summer monsoon season due to rainy washout (majorly) and higher mixing layer (secondarily). Despite the fact that the April–August period is characterized by higher levels of dust over IGP, the dust plumes mostly travel at elevated layers (Komppula et al., 2011) without directly affecting $PM_{2.5}$ concentrations in the ground. However, on certain days in pre-monsoon, $PM_{2.5}$ can reach above 300 μg m^{-3} associated with dust storms and/or wheat crop-residue burning, but the most important finding is the dramatic increase in $PM_{2.5}$ concentrations in October and November (Fig. 1a). This is attributed to the extensive agricultural biomass burning over Punjab in that season resulting in severe AODs (>1.5) over the whole IGP and $PM_{2.5}$ levels above 150–200 μg m^{-3} in Patiala, Punjab (Kaskaoutis et al., 2014).

Offline (gravimetric technique) $PM_{2.5}$ samples were collected and analysed over Delhi during day (10:00–18:00 h) and night (19:00–07:00 h) times. Following this method, which lacks of high temporal resolution, the annual-mean $PM_{2.5}$ mass concentrations were found to be 164.2 ± 39.9 μg m^{-3} and 179.0 ± 64.8 μg m^{-3} during day and night hours, respectively corresponding to an annual mean of 171.6 ± 51.6 μg m^{-3}, which is ~27% higher than that of the online concentrations. Similarly, the offline daytime and night-time concentrations were found to be 38% and 28% higher than the respective online values of 103.8 ± 57.9 μg m^{-3} and 129.4 ± 90.6 μg m^{-3}. This difference is attributed to the blockage of the filter porous in the Beta-attenuation analyser (Tiwari et al., 2014c) due to high particle loading over Delhi. Fig. 2 summarizes the monthly-mean variations of the online and offline $PM_{2.5}$ mass concentrations over Delhi, separating them for daytime and night-time. Both methods agree to a similar annual pattern of low $PM_{2.5}$ concentrations during monsoon and much larger during post-monsoon and winter (Table 1), but with significant differences in the $PM_{2.5}$ concentrations. These differences are attributed to the various instrumentation and techniques used, the blockage of the filter porous, as well as to the different temporal resolution of the measuring protocols. The latter seems to be the most important factor, since the offline measurements were taken on about 4 days per month and may not be so representative of the monthly average, especially for months with high $PM_{2.5}$ variability. Note also that in months with the highest $PM_{2.5}$ (Oct–Jan), the differences are smaller (~15%). Severe turbid atmospheres with excess of 200 μg m^{-3} were found at 16% (42%) of the days for online (offline) $PM_{2.5}$ measurements. These exceedances are mostly observed in November (15%), December (11%) and January (16%) causing serious concerns in human health. In contrast, the rainy washout during monsoon lowers the $PM_{2.5}$ concentrations from the one hand and, from the other, leads to inhomogeneity that affects the gravimetric $PM_{2.5}$ measurements resulting in differences as high as 100–130% (in August and September) between the two methods.

The annual $PM_{2.5}$ variability over Delhi is attributed to seasonally-changed meteorological conditions and reversible monsoon circulation, rainy washout during monsoon, changes in local and regional anthropogenic emission rates, influence of the long-range transported dust and biomass smoke and evolution of boundary-layer height (BLH), which plays a crucial role in accumulation and dispersion of aerosol and pollutants (Badarinath et al., 2009; Hyvärinen et al., 2011).

4.2. Carbonaceous aerosols

Fig. 3 shows the monthly-mean variations of OC and EC mass concentrations as well as OC/EC (daytime and night-time) obtained via the gravimetric method. On annual basis, the mean OC concentration was found to be 34.1 ± 11.7 μg m^{-3} (daytime) and 41.4 ± 17.6 μg m^{-3} (night-time), corresponding to an annual mean of 37.7 ± 14.3, while the respective EC masses are 5.3 ± 2.3 μg m^{-3} and 10.3 ± 5.7 μg m^{-3}. These are similar to the BC mass concentrations (5.2 ± 3.8 μg m^{-3} for daytime and 10.6 ± 6.7 μg m^{-3} for night-time) obtained via Aethalometer (see Fig. 4). On annual basis, the night-time OC concentration is ~23% higher than the daytime one, whereas the night-time EC is double than that in daytime. Similar results were also found in previous studies over Delhi (Pipal et al., 2014b; Tiwari et al., 2013a). A reverse situation is observed in September, when the night-time OC and EC concentrations are lower by ~3% and ~13%, respectively. In September, as well as during the whole monsoon season, the daily variability of carbonaceous aerosols flattens out, as was also shown for $PM_{2.5}$ (Fig. 2). The abundance of EC during night-time is much more favoured by the primary emissions from bio-fuel combustion in Delhi (Srivastava et al., 2014), while the similarity in OC concentrations between day and night during the hot period (April–September) is attributed to the increased SOC formation during daytime as a result of high insulation within a humid polluted environment (Presto et al., 2005a,b). Furthermore, the rainy washout and the better atmospheric mixing and dilution processes within a windy, turbulent

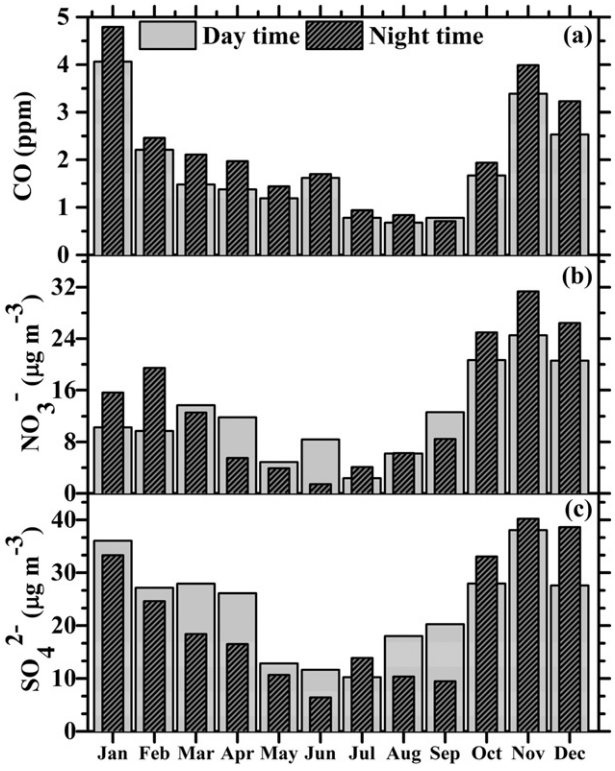

Fig. 5. Monthly-mean concentrations of ionic species (SO_4^{2-} and NO_3^-) and CO over Delhi during day and night.

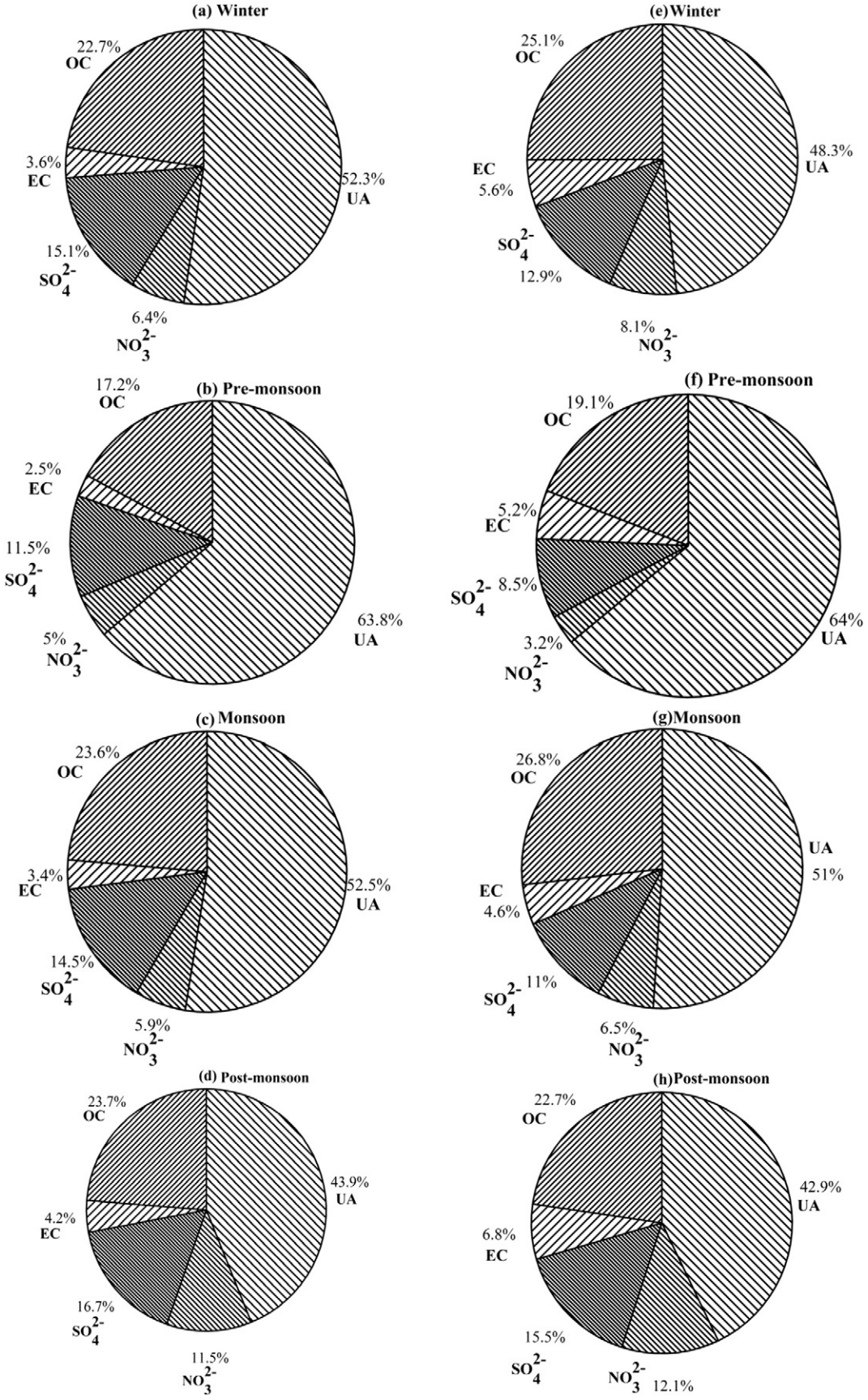

Fig. 6. Seasonal mean percentage contribution of EC, OC and ionic species in the $PM_{2.5}$ during day and night.

and thick mixing layer during monsoon lead to smooth diurnal OC and EC patterns.

In general, the annual variations of OC and EC follow that of $PM_{2.5}$ (Fig. 2), suggesting that carbonaceous aerosols are major components of the fine particulate. The seasonally-averaged OC and EC concentrations (Table 1) render Delhi as one of the most carbonaceous aerosol-laden environments in India (Beegum et al., 2009; Goto et al., 2011). In March and November the EC concentrations are higher by ~37% and ~52%, respectively than the annual mean, mostly due to the influence of long-range transport of soot aerosols from wheat crop-residue burning (Kumar et al., 2011) along with fires in Himalayan foothills (Vadrevu et al., 2012) in pre-monsoon and rise crop-residue burning during post-monsoon (Singh and Kaskaoutis, 2014). Agricultural burning occurs mostly in the states of Punjab and Haryana (Awasthi et al., 2011), which are situated in the northwest upwind direction of Delhi.

OC/EC is an important diagnostic index for identification of the source strength of carbonaceous aerosols (from fossil fuel and/or biofuel combustion) and has significant importance in radiative properties (Carrico et al., 2003; Ram and Sarin, 2011). OC/EC is mostly affected by the fuel type, combustion efficiency, biogenic emissions, formation of Secondary Organic Aerosol (SOA) and different removal rates (Cachier et al., 1996; Turpin and Lim, 2001), while it constitutes an important input in radiative transfer models for estimates of radiative forcing (Bond et al., 2013; Safai et al., 2014).

Higher OC/EC (Fig. 3, secondary y-axis) values dominate during daytime throughout the year (except of September) due to favouring in formation of SOC (Tiwari et al., 2014c). On annual base, OC/EC was found to be 7.09 and 4.55 during day and night, respectively with monthly ranges of 5.2–9.2 (day) and 2.9–8.2 (night). The rather complicated annual variation of OC/EC for both daytime and night-time observations does not allow the extraction of a safe conclusion about emission sources and dominance in contribution of fossil-fuel or biofuel combustions. However, during the severe agricultural burning period of Oct–Nov 2012 (Kaskaoutis et al., 2014), OC/EC seems to be lower (<5.0 on average), while during the wheat crop-residue burning in April–May, the above 6.0 OC/EC values indicate higher SOA formation during daytime (Fig. 3). The contrasting factors that affect the ratio prevent us from extracting a clear differentiation of the carbonaceous aerosol sources and combustion processes (agricultural biomass burning, biofuel combustion, vehicular exhausts) over Delhi (Ram and Sarin, 2010; Pipal et al., 2014a; Tiwari et al., 2014c). However, the seasonal-mean OC/EC is larger during monsoon (Table 1), in accordance with previous results at Nainital, central Indian Himalayas (Ram et al., 2010). The OC/EC at Nainital was found to be slightly higher than that obtained in Delhi (Table 2) due to a lesser impacted environment from automobiles and industry exhausts that, in general, increase the emissions of EC against to OC. Chow et al. (1996) and Safai et al. (2014) suggested that a ratio greater than 2.0 indicates SOA formation. Schauer et al. (2002) reported OC/EC values of 1.0–4.2 and 16.8–40.0 for diesel/gasoline-powered vehicular exhausts and wood combustion, respectively, while similar results were found by Saarikoski et al. (2008) with OC/EC values of 6.6 (biomass burning) and 0.71 (vehicular emissions) and Watson et al.

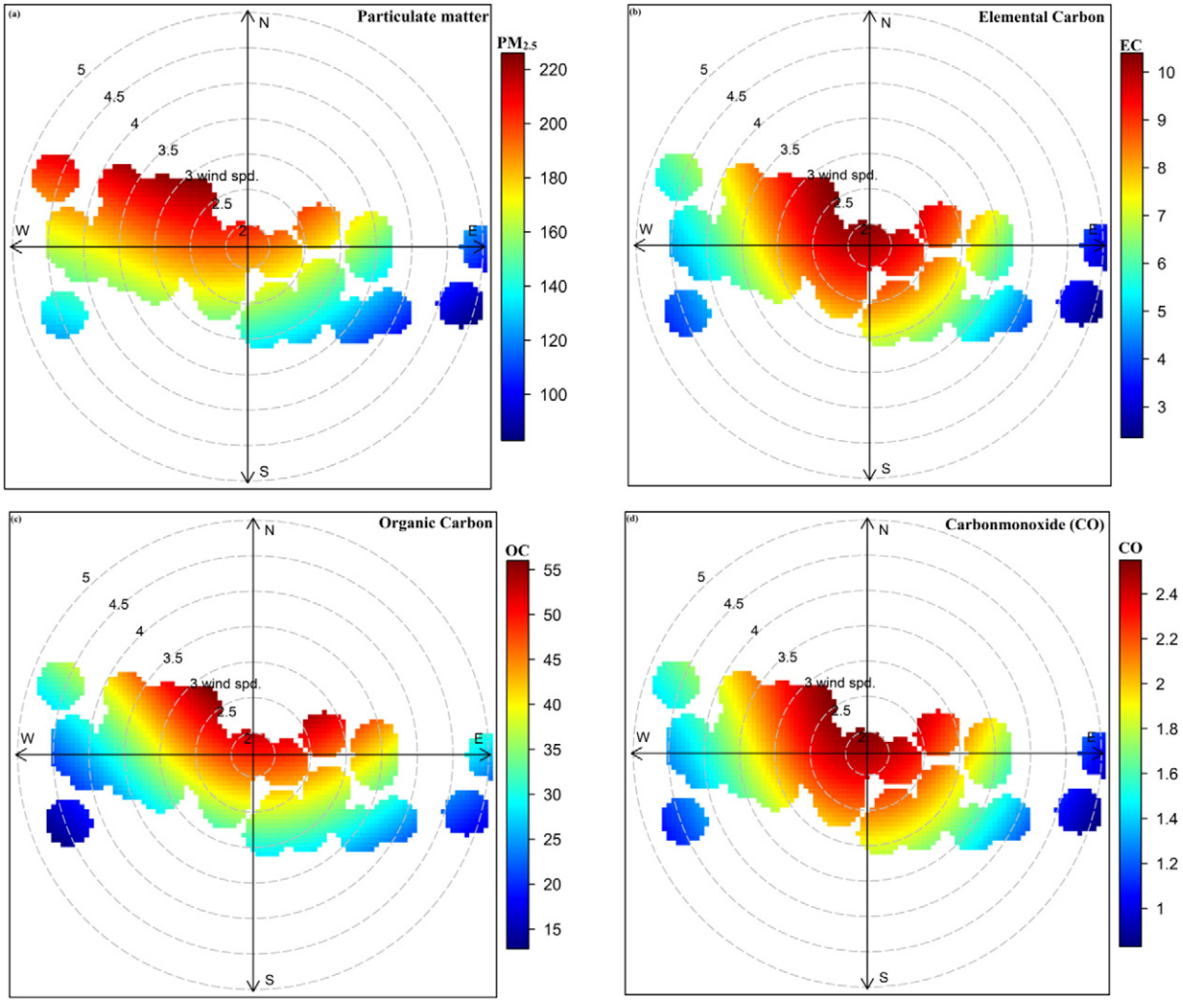

Fig. 7. Bivariate plots of $PM_{2.5}$ (a), EC (b), OC (c) and CO (d) over Delhi during Jan–Dec 2012.

(2001) with OC/EC of 14.5 for forest fires. OC/EC of 4.1 for vehicle exhausts, 12.0 for coal combustion, and 60.3 for biomass burning were reported over Xi'an, China (Cao et al., 2005). The correlation coefficients between OC and EC concentrations were found to be 0.82 (day) and 0.81 (night), indicating common combustion sources, despite the significant variability in emissions from diesel, petrol and wood combustion.

The monthly-mean variation of the BC mass concentrations obtained via Aethalometer measurements (Fig. 4), shows a similar pattern to that of EC with late post-monsoon and winter maximum and monsoon minimum (Table 1). The severe agricultural burning in Oct–Nov 2012 exhibits a strong signal in the BC mass concentrations (>18 μg m^{-3} during night), while the similar magnitude in March is well coincident with that obtained for EC (Fig. 3). The results show considerably higher night-time concentrations due to the confinement of the mixing height and trapping of pollutants near the ground. The comparison between BC and EC mass concentrations (Fig. 4 inset) indicates a rather satisfactory agreement between the different instrumentation and techniques ($R^2 = 0.65$, Mean Bias Deviation (MBD) = 0.02 and Root Mean Square Deviation (RMSD) = 3.23%), despite the difference in the temporal resolution and number of averaging data. However, in few cases the differences in mass concentration may increase up to 5 μg m^{-3} or ~20–30% (or even more) with a random distribution along the seasons (Table 1).

4.3. Pollutants (CO, NO_3^- and SO_4^{2-})

Gaseous pollutants, such as CO produced by incomplete combustion of fossil and biofuels and acidic species (nitrate: NO_3^- and sulphate: SO_4^{2-}), were also measured during day and night. The acidic species are produced by the oxidation of gaseous precursors (SO_2 and NO_x) in the atmosphere via photochemical activity under certain conditions of high temperature and humidity, lowering the air ventilation and enhancing the photochemistry at regional scale (Hidy, 1994; Zhang et al., 2012). Fig. 5a–c shows the monthly concentrations of CO, NO_3^- and SO_4^{2-}, respectively, which seem to follow the annual pattern of $PM_{2.5}$ with larger values during post-monsoon and winter and lower in monsoon (for the same reasons discussed above). The average concentrations of CO are 1.99 ppm and 2.39 ppm during day and night, respectively with the daytime concentration to meet the NAAQS and the night-time one to be ~20% higher. The highest concentrations of NO_3^- (20–30 μg m^{-3}) are found during the severe Oct–Nov 2012 agricultural biomass-burning period, when large amounts (8–9 × 10^{15} mol cm^{-2}) of NO_2 were detected via OMI sensor over northwestern IGP (Kaskaoutis et al., 2014). The annual-averaged NO_3^- and SO_4^{2-} concentrations were found to be 12.3 μg m^{-3} and 25.0 μg m^{-3} during daytime and 13.8 and 22.4 μg m^{-3} during night-time. From March to September the daytime concentrations dominate, while during the rest of the year NO_3^- and SO_4^{2-} are more abundant during night-time (except of SO_4^{2-} during Jan–Feb), while the CO concentration is always larger during night-time. Larger SO_4^{2-} and NO_3^- concentrations during daytime may be due to excess of photochemical formation in addition to local emissions during the rush hours, while the low-mixing layer during night-time seems to be the most responsible factor for the higher concentrations along with additional emissions from biofuel and waste-material burning for heating purposes during winter (Shaiganfar et al., 2011).

The particulate SO_4^{2-} and NO_3^- are produced from their precursor gases through chemical transformation processes in the atmosphere, which are mostly associated with the fine mode (Seinfeld and Pandis, 1998). Furthermore, NO_3^- facilitates the oxidation of volatile organic

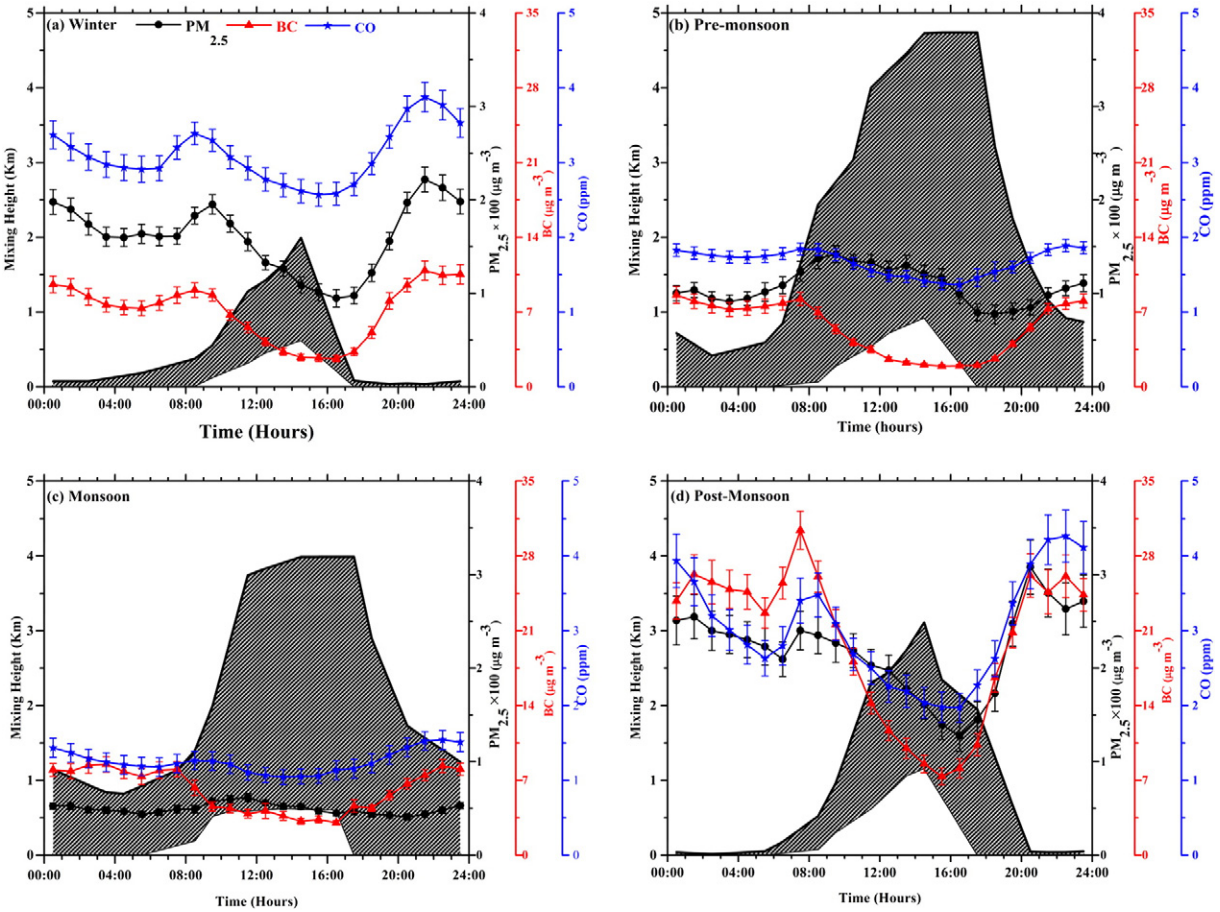

Fig. 8. Diurnal variation of the seasonal mean $PM_{2.5}$, BC and CO concentrations along with respective variations in the maximum and minimum mixing layer height layer over Delhi.

compounds to form SOA due to photochemical formation during daytime (Rastogi et al., 2014). On the other hand, the highest concentration of NO_3^- during winter may be attributed to the atmospheric stability and formation of ammonium nitrate (NH_4NO_3) aerosols at low temperatures as well as to heterogeneous formation of NO_3^- via hydrolysis of N_2O_5 under high humidity conditions (Guo et al., 2010; Behera and Sharma, 2010).

Fig. 6 summarizes the contributions of the carbonaceous aerosols and acidic species in the $PM_{2.5}$ mass (offline measurements) on seasonal basis for both daytime and night-time observations in Delhi. The main findings consist of the larger fraction of carbonaceous aerosols during night, the increase of EC in winter and post-monsoon and the significant contribution of OC during monsoon due to SOA formation. As a major component of industrial emissions, SO_4^{2-} exhibits similar contributions to $PM_{2.5}$ in all seasons with slightly higher values during daytime, while NO_3^- significantly increases during post-monsoon due to severe agricultural biomass burning in Punjab. Taking into account the mean NO_3^- contributions of ~4–8% during the rest of the year, the 11.5–12% found in post-monsoon suggests an increase in the order of 40–60% due to transported smoke. The contribution of the carbonaceous aerosols and acidic species to the $PM_{2.5}$ mass is much lower during pre-monsoon (36%) due to enhancement in dust component and quoting that modifies aerosol properties (Singh et al., 2010; Srivastava et al., 2011). The analysis showed that the acidic species exhibit a good correlation with $PM_{2.5}$ with R^2 of 0.51 for NO_3^- and 0.67 for SO_4^{2-}, respectively suggesting more or less common sources and important contribution to $PM_{2.5}$. Sharma and Kulshrestha (2014) also reported a strong correlation of $R^2 = 0.79$ between NO_2 and AOD over urban areas in India, whereas the respective correlation with SO_2 was not so significant. They explained it in the view of emission sources, since the vehicular emissions are a common source of PM and NO_2, while SO_2 is mostly emitted by fossil-fuel burning (Pan et al., 2014).

4.4. Role of meteorology, boundary-layer dynamics and long-range transport

The natural and anthropogenic emissions from local to regional scales and the seasonally-changed meteorological parameters control the variability of aerosol over Delhi. The role of wind (speed and direction) on $PM_{2.5}$, OC, EC and CO concentrations is examined via the bivariate polar graphs with size bins of 1 ms^{-1} and 10° for wind speed and direction, respectively (Fig. 7 a–d). The meteorological data were obtained from India Meteorological Department (IMD), New Delhi.

In general, the analysis reveals that the west/northwest flow enhances all the concentrations, which are mostly associated with low wind speeds (calm to ~3 ms^{-1}) indicating that the severe turbid/polluted atmospheres over Delhi are much more favoured by low northwestern winds. These meteorological conditions contribute to accumulation of aerosol and pollutants within Delhi and/or to additional transport from polluted regions in northwest, like urban Lahore and agricultural burning in Punjab. In contrast, higher (5 ms^{-1}) easterlies, associated with the monsoonal circulation and rainfall, seem to act as ventilation tool for urban environment. The $PM_{2.5}$ bivariate plot does not reveal any important contribution of dust coming from the west-southwest directions (Lodhi et al., 2013). Dust activity was rather low during the 2012 pre-monsoon season with few cases of severe $PM_{2.5}$ (Fig. 1). On the other hand, major pollution sources, like thermal power plants and industrial belts located in the upwind or downwind directions of a measuring site, may strongly affect the bivariate plots; however,

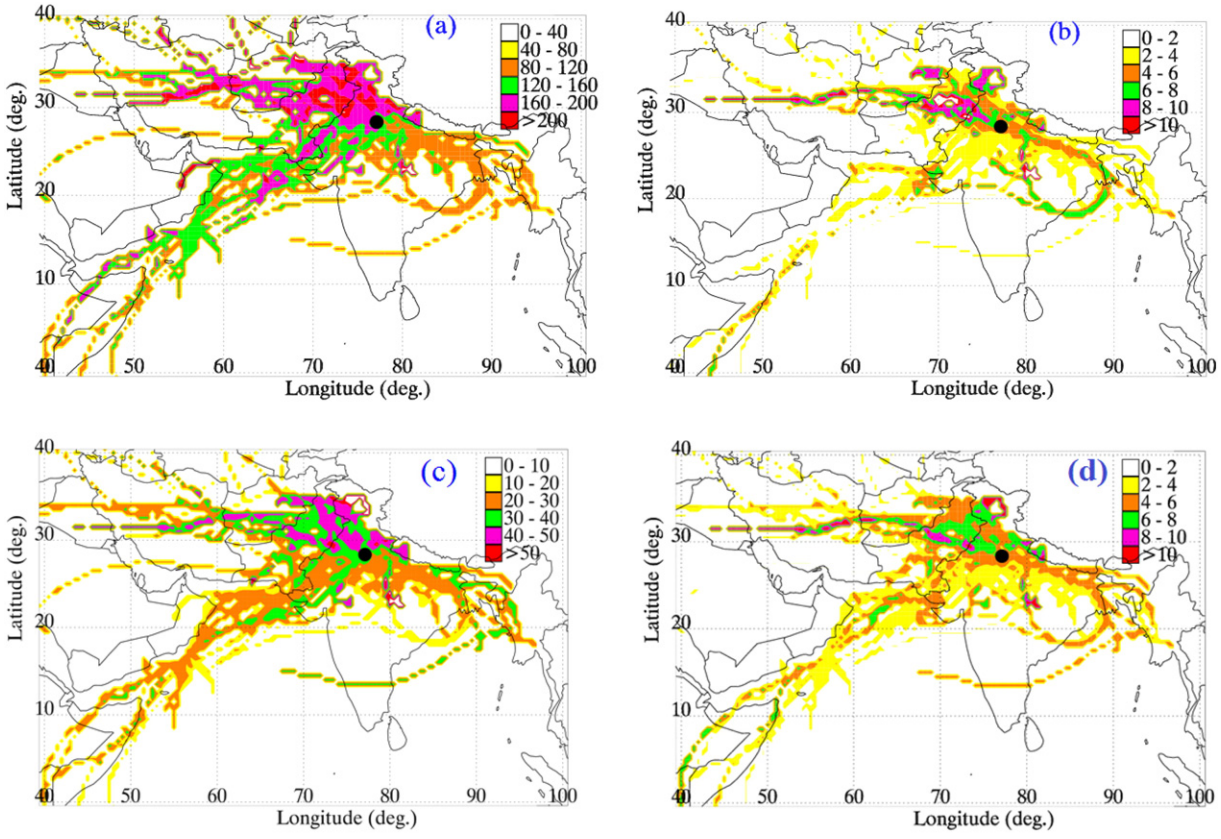

Fig. 9. Concentration weighted trajectory (CWT) maps using 5-day air-mass back trajectories ending at 500 m above ground level for $PM_{2.5}$ (a), BC (b), OC (c) and EC (d) mass concentrations. The black circle denotes Delhi.

Table 3
Number of trajectories and concentrations of $PM_{2.5}$, OC, EC, SO_4^{2-}, NO_3^-, BC and CO for each cluster (see text for details).

Clusters Group	No. of Airmass trajectory	$PM_{2.5}$	OC (μg m^{-3})	EC (μg m^{-3})	SO_4^{2-} (μg m^{-3})	NO_3^-(μg m^{-3})	BC (μg m^{-3})	CO (ppm)
1	10	117.55 ± 49.07	30.02 ± 14.50	04.94 ± 2.22	15.79 ± 10.43	8.62 ± 05.33	6.12 ± 3.94	1.13 ± 0.75
2	52	205.65 ± 55.04	48.52 ± 15.55	10.10 ± 5.53	29.13 ± 13.80	16.16 ± 10.71	10.49 ± 7.11	2.88 ± 1.49
3	11	161.08 ± 44.79	28.03 ± 10.00	05.62 ± 3.63	21.52 ± 13.26	10.95 ± 09.52	4.50 ± 3.50	1.48 ± 0.69
4	17	139.19 ± 34.92	22.81 ± 07.55	04.88 ± 3.33	13.57 ± 08.80	06.66 ± 07.52	3.91 ± 3.64	1.18 ± 0.64

such a large contribution from a preferential sector within Delhi urban environment does not exist and the vehicular and industrial/urban emissions are from all directions throughout the year. Thus, for calm atmospheres, the $PM_{2.5}$ and carbonaceous aerosol concentrations are high and nearly independent from the direction, while for light and moderate winds the northwestern flow carries additional aerosol and smoke plumes during post-monsoon and winter (Mishra and Shibata, 2012).

Fig. 8 shows the seasonal-mean diurnal evolution of $PM_{2.5}$, BC and CO along with that of BLH (max and min values) as obtained in hourly basis from HYSPLIT model using the Turbulent Kinetic Energy (TKE) profile method (Draxler et al., 2014; Dumka et al., 2015; http://ready.arl.noaa.gov/HYSPLIT.php), supposing that the BLH is assigned to the height at which TKE either decreases by a factor of two or to a value less than 0.21 (m^2/s^2). BLH exhibits a pronounced diurnal variation in all seasons, especially in pre-monsoon, when it reaches up to 4.5 km in early-afternoon. During night-time and early morning, BLH is only a few metres trapping aerosols and pollutants near the ground, thus controlling the diurnal variation of carbonaceous aerosol and $PM_{2.5}$ and favouring the formation of haze and fog during the late post-monsoon and winter (Komppula et al., 2011).

Taking into account that the local anthropogenic emissions are continuous within Delhi urban environment without a strong annual variation, except for the increased biofuel and waste burning during winter for heating purposes, the diurnal (majorly) and seasonal (secondarily) patterns of the $PM_{2.5}$ and carbonaceous aerosol concentrations are mostly controlled by the boundary-layer dynamics. Therefore, during post-monsoon, winter and night-time when the BLH is very low the concentrations are highest, in contrast to the lower ones during noon associated with maximum BLH and, therefore, better dilution. The diurnal pattern seems to smooth during monsoon mostly due to rainy washout processes. Similar diurnal patterns of near-surface aerosol and BC were reported over Delhi and other urban environments around India (Ganguly et al., 2006; Beegum et al., 2009), thus highlighting the role of boundary-layer dynamics. The absence of a distinct $PM_{2.5}$ diurnal cycle during pre-monsoon may be attributed to the strong contribution of re-suspended dust on the $PM_{2.5}$ mass during the rush hours (morning to noon), while the long-range transport (LRT) seems to play an important role in the high values and diurnal variability during post-monsoon.

For identifying the role of LRT we examine the potential sources that contribute to the aerosol and pollution concentrations over Delhi via the CWT analysis (Fig. 9a–d). The analysis reveals that the hot spot areas responsible for high $PM_{2.5}$ concentrations (>200 μg m^{-3}) are located in the northwest IGP and central Pakistan (Fig. 9a). Furthermore, arid terrain in Iran–Afghanistan seems to further contribute to high $PM_{2.5}$ levels on certain circumstances (dust transport), while the contribution of the local domain is also important. Southwest air masses from Arabian Sea carrying a mixing of dust and marine aerosols (Lodhi et al., 2013) seem to contribute to moderate-to-high $PM_{2.5}$ concentrations, while trajectories from the eastern IGP (most frequent during monsoon) are associated with lower $PM_{2.5}$ concentrations. The CWT map for $PM_{2.5}$ is similar to that reported by Lodhi et al. (2013) for the columnar AOD; however, on Lodhi's case the contribution of the southwest sector was larger due to dust transport at elevated heights during the pre-monsoon and monsoon seasons. In contrast, in the case of carbonaceous aerosols (Fig. 9b, c, d), the southwest sector contributes only a little, while the main hot-spot areas remain the northwest IGP (agricultural burning) and central-north Pakistan. Eastern air masses may also contribute to the carbonaceous aerosol, but with much lesser intensity. The CWT maps for ionic species ($NO3^-$ and $SO4^{2-}$) and CO are shown in supplementary Fig. S-1.

Via the cluster analysis technique (Dumka et al., 2013) the air-mass back trajectories were classified into 4 groups (sectors) which are examined separately in view of aerosol concentrations (Table 3 and Supplementary Fig. S-2). The identified groups are: Cluster 1 (11% of the cases), which accounts for air masses coming from eastern IGP, Cluster 2 (58%) defining the local-regional sector and air masses from the northwestern IGP, Cluster 3 (12%) for air masses coming from long distances (SW Asia and Middle East) and Cluster 4 (19%) associated with air masses from the Arabian Sea (southwest sector). The highest

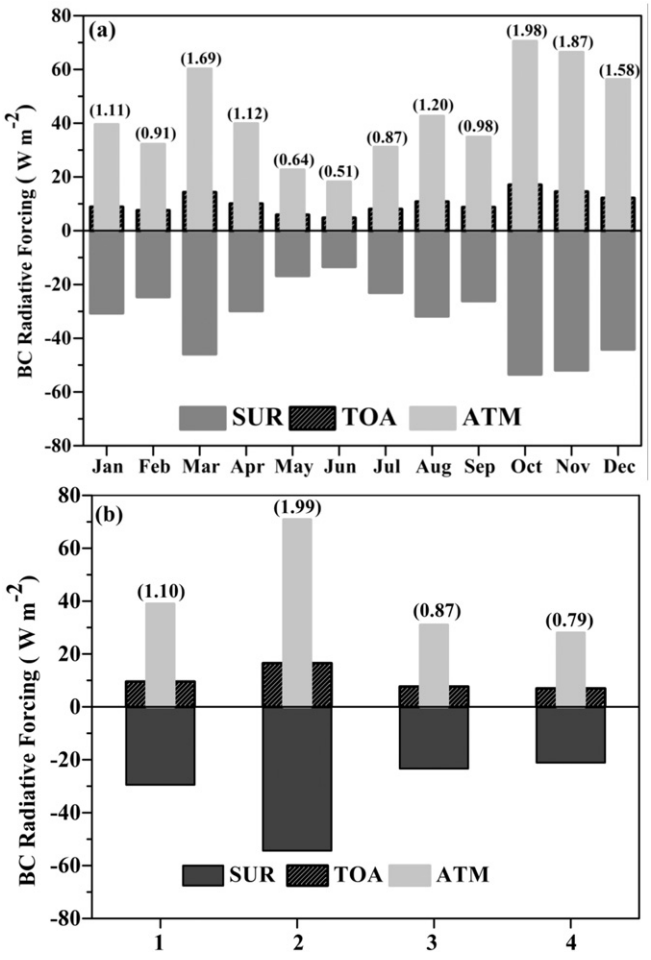

Fig. 10. (a) Monthly variation of BC DRF at top of the atmosphere (TOA), surface (SUR) and atmosphere (ATM) and corresponding heating rates (HR) in parentheses over Delhi. (b) BC DRF and HR values classified to each cluster (see text for details).

concentrations for all variables are associated with Cluster 2, which were found to be 75%, 48% and 28% higher (in the case of $PM_{2.5}$) than those of Clusters 3, 4 and 1, respectively. This indicates that the local and regional sources (mostly anthropogenic) contribute to the highest $PM_{2.5}$ levels in Delhi, also associated with almost double concentrations of carbonaceous aerosols (Table 3).

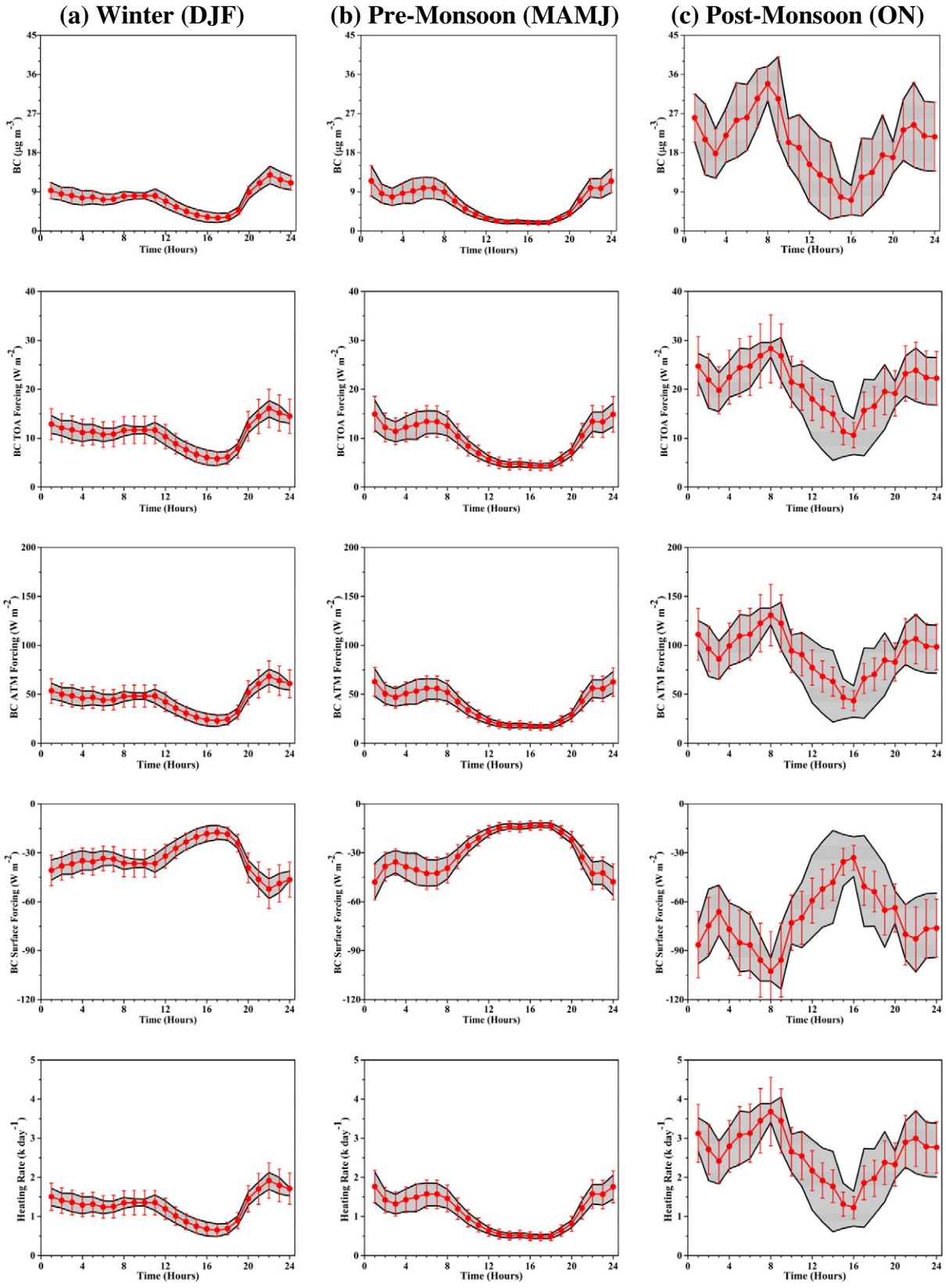

Fig. 11. Diurnal variation of hourly averaged BC mass concentration (first raw), TOA DRF (second raw), ATM DRF (third raw), SUR DRF (fourth raw) heating rate (fifth raw) during winter (a), pre-monsoon (b) and post-monsoon (c) seasons (see text for details).

4.5. Radiative impact of BC

SBDART (Santa Barbara Discrete Ordinate Radiative Transfer; Ricchiazzi et al., 1998) model was used for estimations of shortwave (0.3–3 μm) direct radiative forcing (DRF) as well as atmospheric heating rate (HR) of BC aerosol under clear-sky conditions over Delhi. The basic input parameters for the estimations of DRF were i) the spectral aerosol optical depth (AOD), ii) the single scattering albedo (SSA) and iii) the asymmetry factor (g), which were obtained via sun/sky radiometric measurements from IMD's India-Skynet (Tiwari et al., 2015). The sun/sky radiometer retrieves spectral AOD at seven (0.34, 0.38, 0.40, 0.50, 0.675, 0.87 and 1.020 μm) wavelengths and more details about the methodology of retrievals and errors are given elsewhere (Tiwari et al., 2015). The standard mid-latitude summer profiles of temperature and pressure were used, along with surface albedo values obtained from Terra and Aqua MODIS (8-Day Level 3 Global 500 m SIN Grid product, MOD09A1 (Terra) and MYD09A1 (Aqua) at seven (0.469, 0.555, 0.645, 0.859, 1.24, 1.64, and 2.13 μm) wavelengths) and total columnar ozone from Ozone Monitoring Instrument (OMI). The surface reflectance was ~0.17 averaged over the period of observations.

For the BC DRF the externally mixed aerosol types (i.e. water soluble, insoluble and soot) were used in the urban aerosol model as described in Optical Properties of Aerosols and Clouds (OPAC; Hess et al., 1998). The BC number density corresponding to online BC mass concentrations is incorporated in OPAC and number concentrations of water soluble and insoluble aerosols are iteratively adjusted to obtain the best fit (uncertainty within ±5%) between measured and modelled spectral AODs (Srivastava et al., 2012; Sinha et al., 2012). The aerosol optical properties (AOD, SSA and g) were estimated with and without inclusion of BC in OPAC and then are inserted in SBDART. The forcing estimates were performed using the eight radiation streams at hourly intervals for a range of solar zenith angles and, then, the 24-h values were obtained and averaged on daily and monthly basis. For the night-time BC forcing estimates, the daily mean values of AOD and other aerosol properties were used. Further details regarding the estimation of BC DRF are given elsewhere (Das and Jayaraman, 2011; Srivastava et al., 2012; Dumka et al., 2013). The RFs at the top of atmosphere (TOA) and surface (SUR) are defined as the change in the net (down minus up) flux with and without BC. The difference between the TOA and SUR forcings is defined as atmospheric (ATM) BC forcing, which represents the absorbed amount of solar energy that contributes to atmospheric heating. The average heating rate due to ΔF_{ATM} is estimated from the first law of thermodynamics using the hydrostatic Eq. (2):

$$\frac{\partial T}{\partial t} = \frac{g}{C_p}\frac{\Delta F_{ATM}}{\Delta P} \quad (2)$$

Where $\partial T/\partial t$ is the heating rate (HR) in K day^{-1}, g/Cp is the lapse rate (g is the acceleration due to gravity and Cp the specific heat capacity of air at constant pressure = 1006 Jkg^{-1} K^{-1}), ΔF_{ATM} is the atmospheric forcing and ΔP the atmospheric pressure difference (taken ΔP as 300 hPa).

Fig. 10 shows the monthly-averaged BC DRF at SUR, TOA and ATM as well as the HR (in parenthesis) and the corresponding forcing for each Cluster. The ATM forcing due to BC aerosol is very high reaching to 60-70 W m^{-2} in Oct–Dec as well as in March as a result of the severe agricultural burning in post-monsoon 2012. This contributes to TOA heating (7–18 W m^{-2}) in all months, while the high heating rates (1.87 K day^{-1} and 1.989 K day^{-1}) have serious climatic effects concerning the low-mid atmosphere heating over northern India and Tibetan Plateau and retreat of Himalayan glaciers (Kopacz et al., 2010). On Cluster basis, the BC DRF is much higher for Cluster 2 (70 Wm^{-2} in ATM and 2 K day^{-1} in HR), highlighting the serious effects of the agricultural burning in Punjab, despite the generally low contribution of EC in aerosol mass (Fig. 6). The BC forcing for the other clusters is much lower, especially for air-masses coming from Arabian Sea (Cluster 4), which are usually low-loaded with soot aerosols (Fig. 9b).

The diurnal variation of BC DRF and HR was also computed on seasonal-mean basis (Fig. 11). In order to estimate the uncertainty in BC radiative forcing, the model was run with three BC concentrations corresponding to i) mean, ii) mean -1 sigma and, iii) mean + 1 sigma (seasonal mean and standard deviation). The daytime seasonal-mean AODs were used for the night-time computations, while the monsoon season is not considered due to low availability of AOD measurements and increase in bias. The vertical bars represent the standard deviation, while the shaded portion in the figures represents the radiative forcing for BC -1 sigma and BC + 1 sigma. The diurnal variations of radiative forcing and heating rate follow that of BC concentration, thus suggesting much lower dependence on diurnal changes in AOD. Therefore, during early-morning and late-evening hours with peak in BC concentrations the TOA and ATM forcing are higher, whereas the surface forcing is more negative. The much higher BC concentrations during the post-monsoon season result in TOA forcing as high as 10.6–28.3 W m^{-2}, ATM forcing in the range of 43.6–130.9 W m^{-2} and SUR forcing of −102.6 to −33.0 W m^{-2} (instantaneous values). The corresponding heating rates can reach up to 3–4 K day^{-1}, being almost double than those computed in winter and pre-monsoon. The uncertainty in BC DRF can reach up to 100–120% in TOA for a two- to three-fold change in BC concentrations suggesting the necessity for accurate BC measurements and model estimates for satisfactory retrievals of BC climate implications (Ganguly et al., 2012). The diurnal change in HR may reach to 66%, 73% and 67% due to corresponding diurnal changes of 77%, 84% and 79% in BC mass concentrations during winter, pre-monsoon and post-monsoon, respectively. Thus, the BC forcing is very much variable even on daily basis and strongly depends on local emission rates, long-range transport and boundary-layer dynamics which control the diurnal BC pattern and concentrations.

The DRF estimates show that the accumulation of carbonaceous aerosol over northern India has serious radiative impacts, which are in the same magnitude to those of natural aerosols (dust) during the pre-monsoon season (Gautam et al., 2011). Dey and Tripathi (2008) and Srivastava et al. (2012) reported an average anthropogenic contribution of ~71% to the composite aerosol radiative forcing over urban/industrial sites (Delhi, Kanpur) in the IGP. However, external and internal mixing of BC with dust leads to significant uncertainties in the radiative impact estimates (Srivastava and Ramachandran, 2012) at both spatial and temporal scales considering the estimate of BC DRF a real challenge.

5. Summary and conclusions

The present study analysed a year-long (January to December 2012) measurements of near-surface fine particulate matter ($PM_{2.5}$) as well as its carbonaceous aerosol and inorganic constituents (sulphate and nitrate) over Delhi megacity. The whole analysis includes two different datasets of $PM_{2.5}$ and carbonaceous aerosol (EC, BC, OC) concentrations (online and offline) using different instrumentation and retrieval techniques, while it is divided for daytime and night-time observations. The online mean $PM_{2.5}$ concentration was found to be 124.6 ± 87.9 μg m^{-3}, varying from 18.2 to 500.6 μg m^{-3}, which is substantially above the National and International air quality standards. Offline $PM_{2.5}$ concentrations during day and night-time were 170.0 and 186.5 μg m^{-3}, respectively which are 28% and 38% higher than the online ones (103.8 and 129.4 μg m^{-3}, respectively). Online BC mass concentrations were similar to the offline EC (~5.3 μg m^{-3} during daytime and ~10.3 μg m^{-3} during night-time). Similar diurnal pattern was found for the OC, with ~23% larger concentrations during night-time. The diurnal pattern of carbonaceous aerosols strongly depends on season, with a clear night-time dominance during post-monsoon and winter, especially for the BC and EC components. The daytime vs night-time differences flattened out in monsoon, while in several cases during the hot period of the year (April–September) the daytime

OC was found to be larger due to favourable meteorological conditions for secondary organic aerosols formation. The rainfall washout and the better mixing into a thick and turbulent boundary layer during monsoon are the main reasons for the weakening of the diurnal pattern of $PM_{2.5}$ and carbonaceous aerosols. The OC/EC was found to be 7.09 and 4.55 for daytime and night-time observations, respectively indicating formation of secondary organic aerosols during daytime. The annual-average concentrations of NO_3^- and SO_4^{2-} were 12.3 and 25.0 μg m^{-3} (13.8 and 22.4 μg m^{-3}) during daytime (night-time). Their contribution to $PM_{2.5}$ mass was seasonally dependent and reached to a maximum of ~16% in post-monsoon. The accumulation of $PM_{2.5}$ and carbonaceous aerosol over Delhi was favoured under low (<3 m s^{-1}) wind speeds from northwestern directions indicating high local-to-regional contribution and strong influence of the Punjab agricultural biomass burning during post-monsoon. Estimates of the BC direct radiative forcing (DRF) showed a large contribution to the TOA warming, which maximized (~18 W m^{-2}) during post-monsoon resulting in atmospheric heating rates up to 1.9–2.0 K day^{-1}. The BC DRF over Delhi was found to be larger for air masses traversing northwestern India, Indus Basin and Punjab, which were identified via the CWT analysis as the carbonaceous aerosol hot-spot areas. The sensitivity of the BC DRF to diurnal and seasonal changes in the BC concentrations and boundary-layer dynamics was significant resulting in uncertainties as high as 100–120% for a 2–3-fold change in the BC mass.

Acknowledgement

The authors gratefully thank Director IITM Pune for providing the infrastructure and encouragements during the study period. Furthermore, the authors gratefully acknowledge the NOAA Air Resources Laboratory (ARL) for the provision of the HYSPLIT transport and dispersion model via READY website (http://www.ready.noaa.gov) that was used for the computation of the CWT analysis.

Appendix A. Supplementary data

Supplementary data to this article can be found online at http://dx.doi.org/10.1016/j.scitotenv.2015.03.083.

References

Ancelet, T., Davy, P.K., Trompetter, W.J., Markwitz, A., Weatherburn, D.C., 2013. Carbonaceous aerosols in a wood burning community in rural New Zealand. Atmos. Pollut. Res. 4, 245–249.

Andreae, M., Gelencsér, A., 2006. Black carbon or brown carbon? The nature of light-absorbing carbonaceous aerosols. Atmos. Chem. Phys. 6, 3131–3148.

Awasthi, A.R., Agarwal, S.K., Mittal, N., Singh, K., Gupta, P.K., 2011. Study of size and mass distribution of particulate matter due to crop residue burning with seasonal variation in rural area of Punjab, India. J. Environ. Monit. 13, 1073–1081.

Babu, S.S., Moorthy, K.K., 2002. Aerosol black carbon over a tropical coastal station in India. Geophys. Res. Lett. 29 (23), 2098. http://dx.doi.org/10.1029/2002GL015662.

Badarinath, K.V.S., Sharma, A.R., Kharol, S.K., Prasad, V.K., 2009. Variations in CO, O_3 and black carbon aerosol mass concentrations associated with planetary boundary layer (PBL) over tropical urban environment in India. J. Atmos. Chem. 62, 73–86.

Bahadur, R., Praveen, P.S., Xu, Y.Y., Ramanathan, V., 2012. Solar absorption by elemental and brown carbon determined from spectral observations. Proc. Natl. Acad. Sci. U. S. A. 109, 17366–17371.

Balasubramanian, R., Qian, W.-B., Decesari, S., Facchini, M.C., Fuzzi, S., 2003. Comprehensive characterization of $PM_{2.5}$ aerosols in Singapore. J. Geophys. Res. 108 (D16), 4523. http://dx.doi.org/10.1029/2002JD002517.

Beegum, S.N., Moorthy, K.K., Babu, S.S., Sathesh, S.K., Vinoj, V., Badarinath, K.V.S., Safai, P.D., Devara, P.C.S., Singh, S., Dumka Vinod, U.C., Pant, P., 2009. Spatial distribution of aerosol black carbon over India during pre-monsoon season. Atmos. Environ. 43, 1071–1078.

Behera, S.N., Sharma, M., 2010. Investigating the potential role of ammonia in ion chemistry of fine particulate matter formation for an urban environment. Sci. Total Environ. 408, 3569–3575.

Birch, M.E., Cary, R.A., 1986. Elemental carbon-based method for monitoring occupational exposures to particulate diesel exhaust. Aerosol Sci. Technol. 25, 221–241.

Bisht, D.S., Tiwari, S., Srivastava, A.K., Srivastava, M.K., 2013. Assessment of air quality during 19th Common Wealth Games at Delhi, India. Nat. Hazards 66, 141–154. http://dx.doi.org/10.1007/s11069-012-0349-4.

Bollasina, M.A., Ming, Y., Ramaswamy, V., 2011. Anthropogenic aerosols and the weakening of the South Asian summer monsoon. Science 334, 502–505.

Bond, T.C., et al., 2013. Bounding the role of black carbon in the climate system: a scientific assessment. J. Geophys. Res. Atmos. 118, 5380–5552.

Cachier, H., et al., 1996. African fire particulate emissions and atmospheric influence. Biomass Burning Glob. Chang. 1, 428–440.

Cao, J.J., et al., 2005. Characterization and source apportionment of atmospheric organic and elemental carbon during fall and winter of 2003 in Xi'an, China. Atmos. Chem. Phys. 5, 3127–3137.

Cao, J.J., Lee, S.C., Chow, J.C., Watson, J.G., Ho, K.F., Zhang, R.J., Jin, Z.D., Shen, Z.X., Chen, G.C., Kang, Y.M., Zou, S.C., Zhang, L.Z., Qi, S.H., Dai, M.H., Cheng, Y., Hu, K., 2007. Spatial and Seasonal Distributions of Carbonaceous Aerosols over China 112. http://dx.doi.org/10.1029/2006JD008205.

Carrico, C.M., Bergin, M.H., Shrestha, A.B., Dibb, J.E., Gomes, L., Harris, J.M., 2003. The importance of carbon and mineral dust to seasonal aerosol properties in the Nepal Himalaya. Atmos. Environ. 37, 2811–2824.

Chow, J.C., Watson, J.G., Lu, Z., Lowenthal, D.H., Frazier, C.A., Solomon, P.A., Thuillier, R.H., Magliano, K., 1996. Descriptive analysis of $PM_{2.5}$ and PM_{10} at regionally representative locations during SJVAQS/AUSPEX. Atmos. Environ. 30, 2079–2112.

Chung, C.E., Ramanathan, V., Decremer, D., 2012. Observationally constrained estimates of carbonaceous aerosol radiative forcing. Proc. Natl. Acad. Sci. U. S. A. 109, 11624–11629.

Cowan, T., Cai, W., 2011. The impact of Asian and non-Asian anthropogenic aerosols on 20th century Asian summer monsoon. Geophys. Res. Lett. 38, L11703. http://dx.doi.org/10.1029/2011GL047268.

Das, S.K., Jayaraman, A., 2011. Role of black carbon in aerosol properties and radiative forcing over western India during premonsoon period. Atmos. Res. 102, 320–334. http://dx.doi.org/10.1016/j.atmosres.2011.08.003.

Dey, S., Tripathi, S.N., 2008. Aerosol direct radiative effects over Kanpur in the Indo-Gangetic basin, northern India: long-term (2001–2005) observations and implications to regional climate. J. Geophys. Res. 113, D04212. http://dx.doi.org/10.1029/2007JD009029.

Draxler, R., et al., 2014. HYSPLIT4 user's guide, version 4, report. NOAA, Silver Spring, Md (www.arl.noaa.gov/documents/reports/hysplit_user_guide.pdf).

Duan, J., Tan, J., Cheng, D., Bi, X., Deng, W., Sheng, G., Fu, J., Wong, M.H., 2007. Sources and Characteristics of carbonaceous aerosol in two largest cities in Pearl River Delta Region, China. Atmos. Environ. 41, 2895–2903.

Dumka, U.C., Manchanda, R.K., Sinha, P.R., Sreenivasan, S., Moorthy, K.K., Babu, S.S., 2013. Temporal variability and radiative impact of black carbon aerosol over tropical urban station Hyderabad. J. Atmos. Sol. Terr. Phys. 105–106, 81–90. http://dx.doi.org/10.1016/j.jastp.2013.08.003.

Dumka, U.C., Bhattu, D., Tripathi, S.N., Kaskaoutis, D.G., Madhavan, B.L.M., 2015. Seasonal inhomogeneity in cloud precursors over Gangetic Himalayan region during GVAX campaign. Atmos. Res. 155, 158–175.

Feng, J., Chan, C.K., Fang, M., Hu, M., He, L., Tang, X., 2006. Characteristics of organic matter in $PM_{2.5}$ in Shanghai. Chemosphere 64, 1393–1400.

Feng, Y., Chen, Y., Guo, H., Zhi, G., Xiong, S., Li, J., Sheng, G., Fu, J., 2009. Characteristics of organic carbon in $PM_{2.5}$ samples in Shanghai, China. Atmos. Res. 92, 434–442.

Gadhavi, H.S., Renuka, K., Kiran, V., Ravi, Jayaraman A., Stohl, A., Klimont, Z., Beig, G., 2014. Evaluation of black carbon emission inventories using a Lagrangian dispersion model — a case study over Southern India. Atmos. Chem. Phys. Discuss. 14, 26903–26938.

Ganguly, D., Jayaraman, A., Rajesh, T.A., Gadhavi, H., 2006. Winter time aerosol properties during foggy and non foggy days over urban centre Delhi and their implication for shortwave radiative forcing. J. Geophys. Res. 111. http://dx.doi.org/10.1029/2005JD007029 D15217.

Ganguly, D., Rasch, P.J., Wang, H., Yoon, J.-H., 2012. Climate response of the South Asian monsoon system to anthropogenic aerosols. J. Geophys. Res. 117, D13209. http://dx.doi.org/10.1029/2012JD017508.

Gautam, R., Hsu, N.C., Tsay, S.C., Lau, K.-M., Holben, B.N., Bell, S., Smirnov, A., Li, C., Hansell, R., Ji, Q., Payra, S., Aryal, D., Kayastha, R., Kim, K.M., 2011. Accumulation of aerosols over the Indo-Gangetic plains and southern slopes of the Himalayas: distribution, properties and radiative effects during the 2009 pre-monsoon Season. Atmos. Chem. Phys. 11, 12841–12863.

Goto, D., Takemura, T., Nakajima, T., Badarinath, K.V.S., 2011. Global aerosol model-derived black carbon concentration and single scattering albedo over Indian region and its comparison with ground observations. Atmos. Environ. 45, 3277–3285.

Guo, S., Hu, M., Wang, Z.B., Slanina, J., Zhao, Y.L., 2010. Size-resolved aerosol water-soluble ionic compositions in the summer of Beijing: implication of regional secondary formation. Atmos. Chem. Phys. 10, 947–959. http://dx.doi.org/10.5194/acp-10-947-2010, 2010.

Han, Y.M., Han, Z.W., Cao, J.J., Chow, J.C., Watson, J.G., An, Z.S., Liu, S.X., Zhang, R.J., 2008. Distribution and origin of carbonaceous aerosol over a rural high mountain lake area, Northern China and its transport significance. Atmos. Environ. 42, 2405–2414.

Hansen, J., Sato, M., Ruedy, R., Nazarenko, L., Lacis, A., Schmidt, G.A., Russell, G., Aleinov, I., Bauer, M., Bauer, S., 2005. Efficacy of climate forcings. J. Geophys. Res.-Atmos. 110, D18104.

He, K.B., Yang, F.M., Ma, Y.L., Zhang, Q., Yao, X.H., Chan, C.K., Cadle, S., Chan, T., Mulawa, P., 2001. The characteristics of $PM_{2.5}$ in Beijing. China. Atmos. Environ. 35, 4959–4970.

Hess, M., Koepke, P., Schult, I., 1998. Optical properties of aerosols and clouds: the software package OPAC. Bull. Am. Meteorol. Soc. 79 (5), 831–844.

Hidy, G.M., 1994. Atmospheric sulphur and nitrogen oxides. Academic Press, San Diego CA.

Huang, H., Ho, K.F., Lee, S.C., Tsang, P.K., Ho, Steven Sai Hang, Zou, C.W., Zou, S.C., Cao, J.J., Xu, H.M., 2012. Characteristics of carbonaceous aerosol in $PM_{2.5}$: Pearl Delta River Region. China. Atmos. Res. 104–105, 227–236. http://dx.doi.org/10.1016/j.atmosres.2011.10.016.

Hyvärinen, A.-P., Lihavainen, H., Komppula, M., Sharma, V.P., Kerminen, V.-M., Panwar, T.S., Viisanen, Y., 2009. Continuous measurements of optical properties of

atmospheric aerosols in Mukteshwar, northern India. J. Geophys. Res. 114. http://dx.doi.org/10.1029/2008JD011489 (D08207).
Hyvärinen, A.-P., Raatikainen, T., Brus, D., Komppula, M., Panwar, T.S., Hooda, R.K., Sharma, V.P., Lihavainen, H., 2011. Effect of the summer monsoon on aerosols at two measurement stations in Northern India — part 1: PM and BC concentrations. Atmos. Chem. Phys. 11, 8271–8282.
Kaskaoutis, D.G., Kumar, S., Sharma, D., Singh, R.P., Kharol, S.K., Sharma, M., Singh, A.K., Singh, S., Singh, A., Singh, D., 2014. Effects of crop residue burning on aerosol properties, plume characteristics and long-range transport over northern India. J. Geophys. Res. 119, 5424–5444. http://dx.doi.org/10.1002/2013JD021357.
Kaspari, S.D., Schwikowski, M., Gysel, M., Flanner, M.G., Kang, S., Hou, S., Mayewski, P.A., 2011. Recent increase in black carbon concentrations from a Mt. Everest ice core spanning 1860–2000 A D. Geophys. Res. Lett. 38, L04703. http://dx.doi.org/10.1029/2010GL046096.
Kenny, L.C., Gussman, R., Meyer, M., 2000. Development of a sharp-cut cyclone for ambient aerosol monitoring applications. Aerosol Sci. Technol. 32, 338–358.
Khan, M.F., Shirasuna, Y., Hirano, K., Masunaga, S., 2010. Characterization of PM2.5, P M2.5–10, and PM > 10 in ambient air, Yokohama, Japan. Atmos. Res. http://dx.doi.org/10.1016/j.atmosres.2009.12.009.
Komppula, M., Mielonen, T., Arola, A., Korhonen, K., Lihavainen, H., Hyvärinen, A.-P., Baars, H., Engelmann, R., Althausen, D., Ansmann, A., Müller, D., Panwar, T.S., Hooda, R.K., Sharma, V.P., Kerminen, V.-M., Lehtinen, K.E.J., Viisanen, Y., 2011. One year of Raman-lidar measurements in Gual Pahari EUCAARI site close to New Delhi in India: seasonal characteristics of the aerosol vertical structure. Atmos. Chem. Phys. 12, 4513–4524.
Kopacz, M., Mauzerall, D.L., Wang, J., Leibensperger, E.M., Henze, D.K., Singh, K., 2010. Origin and radiative forcing of black carbon transported to the Himalayas and Tibetan Plateau. Atmos. Chem. Phys. 11, 2837–2852.
Kumar, R., Naja, M., Satheesh, S.K., Ojha, N., Joshi, H., Sarangi, T., Pant, P., Dumka, U.C., Hegde, P., Venkataramani, S., 2011. Influences of the springtime northern Indian biomass burning over the central Himalayas. J. Geophys. Res. 116, D19302. http://dx.doi.org/10.1029/2010JD015509.
Lau, K., Kim, M., Kim, K., 2006. Asian summer monsoon anomalies induced by aerosol direct forcing: the role of the Tibetan Plateau. Clim. Dyn. 26, 855–864.
Lawrence, M.G., Lelieveld, J., 2010. Atmospheric pollutant outflow from southern Asia: a review. Atmos. Chem. Phys. 10, 11017–11096.
Li, W., Bai, Z., 2009. Characteristics of Organic and Elemental Carbon in Atmospheric Fine Particles in Tianjin, China. Particuology 7 (6), 432–437.
Li, H., Feng, J., Sheng, G., Lü, S., Fu, J., Peng, P., Ren, M., 2008. The PCDD/F and PBDD/F pollution in the ambient atmosphere of Shanghai, China. Chemosphere 70, 576–583.
Lin, J.J., 2002. Characterization of the major chemical species in $PM_{2.5}$ in the Kaohsiung City, Taiwan. Atmos. Environ. 36, 1911–1920.
Lodhi, N.K., Beegum, S.N., Singh, S., Kumar, Krishan, 2013. Aerosol climatology at Delhi in the Western Indo Gangetic Plain: microphysics, long-term trends and source strengths. J. Geophys. Res. 118. http://dx.doi.org/10.1002/jgrd.50165.
Lonati, G., Ozgen, S., Giugliano, M., 2007. Primary and secondary carbonaceous species in $PM_{2.5}$ samples in Milan (Italy). Atmos. Environ. 41, 4599–4610.
Meehl, G.A., Arblaster, J.M., Collins, W.D., 2008. Effects of black carbon aerosols on the Indian monsoon. J. Clim. 21, 2869–2882. http://dx.doi.org/10.1175/2008JCLI2362.1.
Menon, S., Koch, D., Beig, G., Sahu, S., Fasullo, J., Orlikowski, D., 2010. Black carbon aerosols and the third polar ice cap. Atmos. Chem. Phys. 10, 4559–4571. http://dx.doi.org/10.5194/acp-10-4559-2010.
Mishra, A.K., Shibata, T., 2012. Climatologically aspects of seasonal variation of aerosol vertical distribution over central Indo-Gangetic belt (IGB) inferred by the space-borne lidar CALIOP. Atmos. Environ. 46, 365–375.
Pachauri, T., Singla, V., Satsangi, A., Lakhani, A., Kumari, K.M., 2013. Characterization of carbonaceous aerosols with special reference to episodic events at Agra, India. Atmos. Res. 128, 98–110.
Pan, X., Chin, M., Gautam, R., Bian, H., Kim, D., Colarco, P.R., Diehl, T.L., Takemura, T., Pozzoli, L., Tsigaridis, K., Bauer, S., Bellouin, N., 2014. A multi-model evaluation of aerosols over South Asia: common problems and possible causes. Atmos. Chem. Phys. Discuss. 14, 19095–19147.
Pandis, S.N., Harley, R.A., Cass, G.R., Seinfeld, J.H., 1992. Secondary organic aerosol formation and transport. Atmos. Environ. 26A, 2269–2282.
Park, S.S., Cho, S.Y., 2011. Tracking sources and behaviours of water-soluble organic carbon in fine particulate matter measured at an urban site in Korea. Atmos. Environ. 45, 60–72.
Pipal, A.S., Jan, R., Bisht, D.S., Srivastava, A.K., Tiwari, S., Taneja, A., 2014a. Day and night variability of atmospheric organic and elemental carbon during winter of 2011–12 in Agra, India. Sustain. Environ. Res. 24 (2), 107–116.
Pipal, A.S., Tiwari, S., Satsangi, P.G., Taneja, A., Bisth, D.S., Srivastava, A.K., Srivastava, M.K., 2014b. Sources and characteristics of carbonaceous aerosols at Agra "World heritage site" and Delhi "capital city of India". Environ. Sci. Pollut. Res. 21, 8678–8691.
Presto, A.A., Huff Hartz, K.E., Donahue, N.M., 2005a. Secondary organic aerosol production from terpene ozonolysis. 1. Effect of UV radiation. Environ. Sci. Technol. 39, 7036–7045.
Presto, A.A., Huff Hartz, K.E., Donahue, N.M., 2005b. Secondary organic aerosol production from terpene ozonolysis. 2. Effect of NOx concentration. Environ. Sci. Technol. 39, 7046–7054.
Ram, K., Sarin, M.M., 2010. Spatio-temporal variability in atmospheric abundances of EC, OC and WSOC over Northern India. J. Aerosol Sci. 41, 88–98.
Ram, K., Sarin, M.M., 2011. Day-night variability of EC, OC, WSOC and inorganic ions in urban environment of Indo-Gangetic Plain: implications to secondary aerosol formation. Atmos. Environ. 45, 460–468.
Ram, Kirpa, Sarin, M.M., 2015. Atmospheric carbonaceous aerosols from Indo-Gangetic Plain and Central Himalaya: impact of anthropogenic sources. J. Environ. Manag. 148, 153–163. http://dx.doi.org/10.1016/j.jenvman.2014.08.015.
Ram, K., Sarin, M.M., Hegde, P., 2010. Long-term record of aerosol optical properties and chemical composition from a high-altitude site (Manora Peak) in Central Himalaya. Atmos. Chem. Phys. 10, 11791–11803. http://dx.doi.org/10.5194/acp-10-11791-2010.
Ram, K., Sarin, M.M., Tripathi, S.N., 2012. Temporal trends in atmospheric $PM_{2.5}$, PM_{10}, elemental carbon, organic carbon, water-soluble organic carbon, and optical properties: impact of biomass burning emissions in the Indo-Gangetic Plain. Environ. Sci. Technol. 46, 686–695.
Ramanathan, V., Carmichael, G., 2008. Global and regional climate changes due to black carbon. Nat. Geosci. 1, 221–227.
Ramanathan, V., et al., 2005. Atmospheric brown clouds: impacts on south Asian climate and hydrological cycle. Proc. Natl. Acad. Sci. U. S. A. 102, 5326–5333.
Ramanathan, V., Ramana, M.V., Roberts, G., Kim, D., Corrigan, C.E., Chung, C.E., Winker, D., 2007. Warming trends in Asia amplified by brown cloud solar absorption. Nature 448, 575–578.
Randles, C.A., Ramaswamy, V., 2008. Absorbing aerosols over Asia: a geophysical fluid dynamics laboratory general circulation model sensitivity study of model response to aerosol optical depth and aerosol absorption. J. Geophys. Res. 113, D21203. http://dx.doi.org/10.1029/2008JD010140.
Rashki, A., Kaskaoutis, D.G., Rautenbach, C.J.dew, Eriksson, P.G., Qiang, M., Gupta, P., 2012. Dust storms and their horizontal dust loading in the Sistan region, Iran. Aeolian Res. 5, 51–62.
Rastogi, N., Singh, A., Singh, D., Sarin, M.M., 2014. Chemical characteristics of $PM_{2.5}$ at a source region of biomass burning emissions: evidence for secondary aerosol formation. Environ. Pollut. 184, 563–569.
Rengarajan, R., Sarin, M.M., Sudheer, A.K., 2007. Carbonaceous and inorganic species in atmospheric aerosols during wintertime over urban and high-altitude sites in North India. J. Geophys. Res. 112, D21307. http://dx.doi.org/10.1029/2006JD008150.
Rengarajan, R., Sudheer, A.K., Sarin, M.M., 2011. Aerosol acidity and secondary organic aerosol formation du ring winter time over urban environment in western India. Atmos. Environ. 45, 1940–1945. http://dx.doi.org/10.1016/j.atmosenv.2011.01.026.
Ricchiazzi, P., Yang, S., Gautier, C., Sowle, D., 1998. SBDART: a research and teaching software tool for plane-parallel radiative transfer in the Earth's atmosphere. Bull. Am. Meteorol. Soc. 79, 2101–2114.
Saarikoski, S., Sillanpaä, M., Saarnio, K., Hillamo, R., Pennanen, A.S., Salonen, R.O., 2008. Impact of biomass combustion on urban fine particulate matter in Central and Northern Europe. Water Air Soil Pollut. 191, 265–277. http://dx.doi.org/10.1007/s11270-008-9623-1.
Safai, P.D., Raju, M.P., Rao, P.S.P., Pandithurai, G., 2014. Characterization of carbonaceous aerosols over the urban tropical location and a new approach to evaluate their climatic importance. Atmos. Environ. 92, 493–500. http://dx.doi.org/10.1016/j.atmosenv.2014.04.055.
Satsangi, A., Pachauri, T., Singla, V., Lakhani, A., Kumari, K.M., 2010. Carbonaceous aerosols at a suburban site in Indo-Gangetic plain. Indian J. Radio Space Phys. 39, 218–222.
Satsangi, A., Pachauri, T., Singla, V., Lakhani, A., Kumari, M.K., 2012. Organic and elemental carbon aerosols at a suburban site. Atmos. Res. 113, 13–21.
Schauer, J.J., Kleeman, M.J., Cass, G.R., Simoneit, B.R.T., 2002. Measurement of emissions from air pollution sources. 5. C1–C32 organic compounds from gasoline-powered motor vehicles. Environ. Sci. Technol. 36, 1169–1180.
See, S.W., Balasubramanian, R., Wang, W., 2006. A study of the physical, chemical, and optical properties of ambient aerosol particles in Southeast Asia during hazy and no hazy days. J. Geophys. Res. 111, D10S08. http://dx.doi.org/10.1029/2005JD006180.
Seibert, P., et al., 1994. Trajectory analysis of aerosol measurements at high alpine sites. In: Borrell, P.M., Cvitas, T., Seiler, W. (Eds.), Transport and Transformation of Pollutants in the Troposphere: Proceedings of EUROTRAC Symposium '94. SPB Acad. Publ., Hague, The Netherlands, pp. 689–693.
Seinfeld, J.H., Pandis, S.N., 1998. Atmospheric chemistry and physics: from air pollution to climate change. Wiley, New York.
Shaiganfar, R., Beirle, S., Sharma, M., Chauhan, A., Singh, R.P., Wagner, T., 2011. Estimation of NOx emissions from Delhi using Car MAX-DOAS observations and comparison with OMI satellite data. Atmos. Chem. Phys. 11, 10871–10887.
Sharma, D., Kulshrestha, U.C., 2014. Spatial and temporal patterns of air pollutants in rural and urban areas of India. Environ. Pollut. 195, 276–281.
Sharma, A.R., Kharol, S.K., Badarinath, K.V.S., Singh, D., 2010. Impact of agriculture crop residue burning on atmospheric aerosol loading — a study over Punjab State, India. Ann. Geophys. 28, 367–379.
Sharma, S.K., Mandal, T.K., Saxena, M., Rashmi, Sharma, A., Datta, A., Saud, T., 2014. Variation of OC, EC, WSIC and trace metals of PM_{10} in Delhi, India. J Atmos Sol Terres Phys. 113, 10–22. http://dx.doi.org/10.1016/j.jastp.2014.02.008.
Singh, R.P., Kaskaoutis, D.G., 2014. Crop residue burning: a threat to South Asian air quality. Eos 95 (37), 333–340.
Singh, S., Soni, K., Bano, T., Tanwar, R.S., Nath, S., Arya, B.C., 2010. Clear-sky direct aerosol radiative forcing variations over mega-city Delhi. Ann. Geophys. 28, 1157–1166.
Sinha, P.R., Dumka, U.C., Manchanda, R.K., Kaskaoutis, D.G., Sreenivasan, S., Krishna Moorthy, K., Suresh Babu, S., 2012. Contrasting aerosol characteristics and radiative forcing over Hyderabad, India due to seasonal meso-scale and synoptic scale processes. Q. J. R. Meteorol. Soc. 139, 434–450. http://dx.doi.org/10.1002/qj.1963.
So, K.L., Guo, H., Li, Y.S., 2007. Long-term variation of $PM_{2.5}$ levels and composition at rural, urban and roadside sites in Hong Kong: increasing impact of regional air pollution. Atmos. Environ. 41, 9427–9434.
Srivastava, R., Ramachandran, S., 2012. The mixing state of aerosols over the Indo-Gangetic Plain and its impact on radiative forcing. Q. J. R. Meteorol. Soc. http://dx.doi.org/10.1002/qj.1958.
Srivastava, A.K., Tiwari, S., Devara, P.C.S., Bisht, D.S., Srivastava Manoj, K., Tripathi, S.N., Goloub, P., Holben, B.N., 2011. Pre-monsoon aerosol characteristics over the Indo-Gangetic Basin: implications to climatic impact. Ann. Geophys. 29, 789–804. http://dx.doi.org/10.5194/angeo-29-789-2011.
Srivastava, A.K., Singh, S., Tiwari, S., Bisht, D.S., 2012. Contribution of anthropogenic aerosols in direct radiative forcing and atmospheric heating rate over Delhi in the Indo-Gangetic Basin. Environ. Sci. Pollut. Res. 19, 1144–1158. http://dx.doi.org/10.1007/s11356-011-0633-y.

Srivastava, A.K., Bisht, D.S., Ram, K., Tiwari, S., Srivastava, M.K., 2014. Characterization of carbonaceous aerosols over Delhi in Ganga basin: seasonal variability and possible sources. Environ. Sci. Pollut. Res. 21, 8610–8619. http://dx.doi.org/10.1007/s11356-014-2660-y.

Stone, E., Schauer, J., Quraishi, T.A., Mahmood, A., 2010. Chemical characterization and source apportionment of fine and coarse particulate matter in Lahore, Pakistan. Atmos. Environ. 44, 1062–1070. http://dx.doi.org/10.1016/j.atmosenv.2009.12.015.

Tiwari, S., Srivastava, A.K., Bisht, D.S., Bano, T., Singh, S., Behura, S., Srivastava, M.K., Chate, D.M., Padmanabhamurty, B., 2009. Black carbon and chemical characteristics of PM_{10} and $PM_{2.5}$ at an urban site of North India. Int. J. Atmos. Chem. 62, 3193–3209.

Tiwari, S., Srivastava, A.K., Bisht, D.S., Bano, T., Singh, S., Behura, S., Srivastava, K.M., Chate, D.M., Padmanabhamurty, B., 2010. Black Carbon and Chemical characteristics of PM_{10} and $PM_{2.5}$ at an urban site of North India. Int. J. Atmos. Chem. 62 (3), 193–209. http://dx.doi.org/10.1007/s10874-010-9148-z.

Tiwari, S., Srivastava, A.K., Bisht, D.S., Safai, P.D., Parmita, P., 2013a. Assessment of carbonaceous aerosol over Delhi in the Indo-Gangetic Basin: characterization, sources and temporal variability. Nat. Hazards 65, 1745–1764.

Tiwari, S., Srivastava, A.K., Bisht, D.S., Parmita, P., Srivastava, M.K., Attri, S.D., 2013b. Diurnal and seasonal variations of black carbon and $PM_{2.5}$ over New Delhi, India: influence of meteorology. Atmos. Res. 125–126, 50–62.

Tiwari, S., Pipal, A.S., Srivastava, A.K., Bisht, D.S., Pandithurai, G., 2014a. Determination of wood burning and fossil fuel contribution of black carbon at Delhi, India using aerosol light absorption technique. Environ. Sci. Pollut. Res. 1–10. http://dx.doi.org/10.1007/s11356-014-3531-2.

Tiwari, S., Bisht, D.S., Srivastava, A.K., Pipal, A.S., Taneja, A., Srivastava, M.K., Attri, S.D., 2014b. Variability in atmospheric particulates and meteorological effects on its mass concentrations over Delhi, India. Atmos. Res. 145–46, 45–56. http://dx.doi.org/10.1016/j. atmosres.2014.03.027.

Tiwari, Suresh, Bisht, D.S., Srivastava, A.K., Gustafsson, Ö., 2014c. Simultaneous measurements of black carbon and $PM_{2.5}$, CO and NOx variability at a locally polluted urban location in India. Nat. Hazards http://dx.doi.org/10.1007/s11069-014-1351-9.

Tiwari, S., Pandithurai, G., Attri, S.D., Srivastava, A.K., Soni, V.K., Bisht, D.S., Anil Kumar, V., Srivastava, M.K., 2015. Aerosol optical properties and their relationship with meteorological parameters during wintertime in Delhi, India. Atmos. Res. 153, 465–479.

Tripathi, S.N., Dey, S., Tare, V., Satheesh, S.K., 2005. Aerosol black carbon radiative forcing at an industrial city in northern India. Geophys. Res. Lett. 32, L08802. http://dx.doi.org/10.1029/2005GL022515.

Turpin, B.J., Huntzicker, J.J., 1995. Identification of secondary organic aerosol episodes and quantification of primary and secondary organic aerosol concentrations during SCAQS. Atmos. Environ. 23, 3527–3544.

Turpin, B.J., Lim, H.J., 2001. Species contributions to $PM_{2.5}$ mass concentrations: revisiting common assumptions for estimating organic mass. Aerosol Sci. Technol. 35, 602–610.

Vadrevu, K.P., Ellicott, E., Giglio, L., Badarinath, K.V.S., Vermote, E., Justice, C., Lau, W.K.M., 2012. Vegetation fires in the Himalayan region — aerosol load, black carbon emissions and smoke plume heights. Atmos. Environ. 47, 241–251.

Venkataraman, C., Habib, G., Eiguren Fernandez, A., Miguel, A.H., Friedlander, S.K., 2005. Residential biofuels in South Asia: carbonaceous aerosol emissions and climate impacts. Science 307, 1454–1456.

Verma, S., Pani, S.K., Bhanja, S.N., 2013. Sources and radiative effects of wintertime black carbon aerosols in an urban atmosphere in east India. Chemosphere 90, 260–269. http://dx.doi.org/10.1016/j.chemosphere.2012.06.063.

Viidanoja, J., Sillanpaä, M., Laakia, J., Kerminen, V.M., Hillamo, R., Aarnio, P., et al., 2002. Organic and black carbon in $PM_{2.5}$ and PM_{10}: 1 year of data from an urban site in Helsinki, Finland. Atmos. Environ. 36 (19), 3183–3193.

Watson, J.G., Chow, J.C., Houck, J.E., 2001. $PM_{2.5}$ chemical source profiles for vehicle exhaust, vegetative burning, geological material, and coal burning in Northwestern Colorado during 1995. Chemosphere 43, 1141–1151.

Yang, H., Yu, J.Z., Ho, S.S.H., Xu, J., Wu, W.-S., Wan, C.H., Wang, X., Wang, L., 2005. The chemical composition of inorganic and carbonaceous materials in $PM_{2.5}$ in Nanjing, China. Atmos. Environ. 39, 3735–3749.

Zhang, X.Y., Wang, Y.Q., Niu, T., Zhang, X.C., Gong, S.L., Zhang, Y.M., Sun, J.Y., 2012. Atmospheric aerosol compositions in China: spatial/temporal variability, chemical signature, regional haze distribution and comparisons with global aerosols. Atmos. Chem. Phys. 12, 779–799.